CCI+ PHASE 1 – NEW ECVS
PERMAFROST

D5.1 CLIMATE ASSESSMENT REPORT (CAR)

VERSION 3.1

19 JANUARY 2022

PREPARED BY

Document Status Sheet

Issue	Date	Details	Authors
1.0	30.10.2019	first version, year 1	I.Nitze, G.Grosse, H.Matthes, H.Wieczorek, A.Bartsch, B.Heim
2.0	30.09.2020	second version: update of service case status and dissemination activities representing year 2	I.Nitze, G.Grosse, H.Matthes, H.Wieczorek, A.Bartsch, B.Heim
2.1	16.10.2020	Inclusion of IPA (represented through Isabelle Gärtner-Roer) evaluation	A. Bartsch
3.0	30.09.2021	update of service case status and dis-semination activities representing year 3	I.Nitze, H.Matthes, H.Wieczorek, S. Lisovksi, B.Heim, A.Bartsch
3.1	19.01.2022	Update (name of cci dataset) in Table 1	A. Bartsch

Author team

Annett Bartsch, B.GEOS

Guido Grosse, AWI

Ingmar Nitze, AWI

Birgit Heim. AWI

Mareike Wieczorek, AWI

Tazio Strozzi, GAMMA

Heidrun Matthes, AWI

Simeon Lisovski, AWI

ESA Technical Officer: Frank Martin Seifert

TABLE OF CONTENTS

EXECUTIVE SUMMARY

Within the European Space Agency (ESA), the Climate Change Initiative (CCI) is a global monitoring program, which aims to provide long-term satellite-based products to serve the climate modelling and climate user community. Permafrost has been selected as one of the Essential Climate Variables (ECVs) which are elaborated during Phase 1 of CCI+ (2018-2021).

There is currently no consistent global Earth Observation-based mapping of the parameters permafrost temperature and active layer thickness as required by GCOS based on Earth Observation records. Permafrost_cci will for the first time provide such information for different epochs and meet the requirements for the production of a climate data record.

The Climate Assessment Report (CAR) summarizes current activities within Permafrost_cci with regard to user requirements defined by the climate modelling user community. User feedback through a workshop, three specific science use cases and a utility assessment are presented in this document.

Use case #1 summaries usage by a regional climate model (HIRHAM). The changing boundary parameters for land has significantly impacted soil temperatures in the model runs. Using all boundary parameters derived from Permafrost_cci and Landcover_cci improved not only the representation of soil temperature but also the representation of air temperature

For use case #2, a comparison of Landsat derived trends separated between fore and non-fire affected areas has been added in this version. Particularly increasing variance within burned areas, with locally strong increase in ALT, may result in triggering further permafrost disturbances. However, more detailed analysis will be conducted to verify/falsify this hypothesis.

A third use case covers a joint study with H2020 Nunataryuk which has a focus on coastal erosion in the Arctic. Derived rates based on Landsat and PALSAR suggest an increase of erosion at study sites in recent years, but uncertainties are also high. However, CRDPv0 ground temperatures at 2 m depth have also been increasing at all these sites between 2003-2017.

Based in result of the PVIR, Permafrost_cci GTD and PFR products for the Northern hemisphere are considered to be most reliable in the permafrost temperature range with GTD < 1°C and in PFR >50% as well as PFR <14% is reliable as non-permafrost.

Recommendations from the 1st user workshop included an increased temporal as well as vertical resolution, specifically regarding climate modelling applications.

1 INTRODUCTION

1.1 Purpose of the document

This document provides the user requirements of climate science and climate services for ECV products of the Permafrost_cci project. The ultimate objective of Permafrost_cci is to develop and deliver permafrost maps as ECV products, primarily derived from satellite-based measurements.

1.2 Structure of the document

The first part of this document provides information on related documents and general permafrost related information. The second part includes information on the products under development.

1.3 Applicable documents

[AD-1] ESA 2017: Climate Change Initiative Extension (CCI+) Phase 1 – New Essential Climate Variables - Statement of Work. ESA-CCI-PRGM-EOPS-SW-17-0032

[AD-2] Requirements for monitoring of permafrost in polar regions - A community white paper in response to the WMO Polar Space Task Group (PSTG), Version 4, 2014-10-09. Austrian Polar Research Institute, Vienna, Austria, 20 pp

[AD-3] ECV 9 Permafrost: assessment report on available methodological standards and guides, 1 Nov 2009, GTOS-62

[AD-4] GCOS-200, the Global Observing System for Climate: Implementation Needs (2016) GCOS Implementation Plan, 2015.

1.4 Reference Documents

[RD-1] van Everdingen, Robert, ed. 1998 revised May 2005. Multi-language glossary of permafrost and related ground-ice terms. Boulder, CO: National Snow and Ice Data Center/World Data Center for Glaciology. (http://nsidc.org/fgdc/glossary/; accessed 23.09.2009)

[RD-2] Bartsch, A., Westermann, Strozzi, T., Wiesmann, A., Kroisleitner, C., 2019: ESA CCI+ Permafrost Product Specifications Document, v1.0

[RD-3] Bartsch, A., Obu, J., Westermann, S., Strozzi, T., 2019: ESA CCI+ Product User Guide (PUG), v1.1

[RD-4] Bartsch, A., Matthes, H., Westermann, S., Heim, B., Pellet, C., Onaca, A., Kroisleitner, C., Strozzi, T., 2019, User Requirements Document (URD), v1.1

[RD-5] Heim, B., Wieczorek, M., Pellet, C., Barboux, C., Delaloye, R., Bartsch, A., Strozzi, T. (2019): ESA CCI+ PVIR, v1.0

[RD-6] Heim, B., Wieczorek, M., Pellet, C., Delaloye, R., Bartsch, A., Strozzi, T. (2020): ESA CCI+ PVIR, v2.0

1.5 Bibliography

A complete bibliographic list that supports arguments or statements made within the current document is provided in Section 6.1.

1.6 Acronyms

A list of acronyms is provided in section 6.2.

1.7 Glossary

The list below provides a selection of terms relevant for the parameters addressed in Permafrost_cci [RD-1]. A comprehensive glossary is available as part of the Product Specifications Document [RD-2].

active-layer thickness

The thickness of the layer of the ground that is subject to annual thawing and freezing in areas underlain by permafrost.

The thickness of the active layer depends on such factors as the ambient air temperature, vegetation, drainage, soil or rock type and total water con-tent, snowcover, and degree and orientation of slope. As a rule, the active layer is thin in the High Arctic (it can be less than 15 cm) and becomes thicker farther south (1 m or more).

The thickness of the active layer can vary from year to year, primarily due to variations in the mean annual air temperature, distribution of soil moisture, and snowcover.

The thickness of the active layer includes the uppermost part of the permafrost wherever either the salinity or clay content of the permafrost allows it to thaw and refreeze annually, even though the material remains cryotic (T < 0°C).

Use of the term "depth to permafrost" as a synonym for the thickness of the active layer is misleading, especially in areas where the active layer is separated from the permafrost by a residual thaw layer, that is, by a thawed or noncryotic (T> 0°C) layer of ground.

REFERENCES: Muller, 1943; Williams, 1965; van Everdingen, 1985

continuous permafrost

Permafrost occurring everywhere beneath the exposed land surface throughout a geographic region with the exception of widely scattered sites, such as newly deposited unconsolidated sediments, where the climate has just begun to impose its influence on the thermal regime of the ground, causing the development of continuous permafrost.

For practical purposes, the existence of small taliks within continuous permafrost has to be recognized. The term, therefore, generally refers to areas where more than 90 percent of the ground surface is underlain by permafrost.

REFERENCE: Brown, 1970.

discontinuous permafrost

Permafrost occurring in some areas beneath the exposed land surface throughout a geographic region where other areas are free of permafrost.

Discontinuous permafrost occurs between the continuous permafrost zone and the southern latitudinal limit of permafrost in lowlands. Depending on the scale of mapping, several subzones can often be distinguished, based on the percentage (or fraction) of the land surface underlain by permafrost, as shown in the following table.

Permafrost	English usage	Russian Usage
Extensive	65-90%	Massive Island
Intermediate	35-65%	Island
Sporadic	10-35%	Sporadic
Isolated Patches	0-10%	-

SYNONYMS: (not recommended) insular permafrost; island permafrost; scattered permafrost.
REFERENCES: Brown, 1970; Kudryavtsev, 1978; Heginbottom, 1984; Heginbottom and Radburn, 1992; Brown et al., 1997.

mean annual ground temperature (MAGT)

Mean annual temperature of the ground at a particular depth.

The mean annual temperature of the ground usually increases with depth below the surface. In some northern areas, however, it is not uncommon to find that the mean annual ground temperature decreases in the upper 50 to 100 metres below the ground surface as a result of past changes in surface and climate conditions. Below that depth, it will increase as a result of the geothermal heat flux from the interior of the earth. The mean annual ground temperature at the depth of zero annual amplitude is often used to assess the thermal regime of the ground at various locations. [RD-1]

permafrost

Ground (soil or rock and included ice and organic material) that remains at or below 0°C for at least two consecutive years .

Permafrost is synonymous with perennially cryotic ground: it is defined on the basis of temperature. It is not necessarily frozen, because the freezing point of the included water may be depressed several degrees below 0°C; moisture in the form of water or ice may or may not be present. In other words, whereas all perennially frozen ground is permafrost, not all permafrost is perennially frozen. Permafrost should not be regarded as permanent, because natural or man-made changes in the climate or terrain may cause the temperature of the ground to rise above 0°C.

Permafrost includes perennial ground ice, but not glacier ice or icings, or bodies of surface water with temperatures perennially below 0°C; it does include man-made perennially frozen ground around or below chilled pipe-lines, hockey arenas, etc.

Russian usage requires the continuous existence of temperatures below 0°C for at least three years, and also the presence of at least some ice.

SYNONYMS: perennially frozen ground, perennially cryotic ground and (not recommended) biennially frozen ground, climafrost, cryic layer, permanently frozen ground.
REFERENCES: Muller, 1943; van Everdingen, 1976; Kudryavtsev, 1978.

2 PRODUCTS GENERATED BY PERMAFROST_CCI

Permafrost_cci is establishing Earth Observation (EO) based products for the permafrost ECV spanning the period from 1997 to 2019. Since ground temperature and seasonal thaw depth cannot be directly observed with space-borne sensors, a variety of satellite and reanalysis data are combined in a ground thermal model to infer these subsurface parameters. The algorithm uses remotely sensed data sets of Land Surface Temperature (MODIS LST/ ESA LST CCI) and landcover (ESA Landcover CCI) to drive the transient permafrost model CryoGrid-3 (CryoGrid-2 in Obu et al., 2019), which yields thaw depth and ground temperature at various depths, while ground temperature then forms the basis for deriving permafrost fraction for a specified location and time.

The version Permafrost Climate Research Data Package (CRDP v2) Version 3.0 of the Climate Research Data Package [RD-3] consists of time series covering the years from 1997 and 2019 for

1. mean annual ground temperature in different depths,
2. active layer thickness (maximum annual active layer depth), and
3. permafrost fraction derived from ground temperature.

3 ASSESSMENT OF PRODUCTS AND OTHER FEEDBACK

3.1 Introduction and Rationale

Warming of the Cryosphere is already exceeding the global average temperature increase and models project further strong warming for these regions (IPCC 2021, IPCC, 2019; IPCC, 2013). Permafrost is an important component of the Cryosphere and defined as ground that remains frozen for at least two consecutive years (Van Everdingen, 1998). Ongoing permafrost warming (Romanovsky et al., 2010; Biskaborn et al., 2019) and near-surface thawing in permafrost regions, associated with rising air temperatures, are considered to reinforce warming of the atmosphere through the partial conversion of the large permafrost soil organic carbon pool into greenhouse gases, a process termed "permafrost carbon feedback" (Schuur et al., 2015). A further challenge for monitoring the impacts of permafrost thaw dynamics is represented by rapid thaw processes that may mobilize a significant amount of carbon over short time spans of years to decades (Turetsky et al., 2019). Worldwide monitoring of permafrost is therefore essential to understand and assess the feedbacks between climate change and permafrost thaw and their impact on the Earth's climate system.

The recently published thorough analysis of global permafrost temperatures by the Global Terrestrial Network for Permafrost (GTN-P) and the International Permafrost Association (IPA) demonstrated that permafrost is warming at a global scale (Biskaborn et al., 2019). This study showed that during the reference decade (2007 to 2016) ground temperature near the depth of zero annual amplitude in the continuous permafrost zone increased by 0.39 ± 0.15 °C. Over the same period, discontinuous permafrost warmed by 0.20 ± 0.10 °C. Permafrost in mountains warmed by 0.19 ± 0.05 °C and in Antarctica by 0.37 ± 0.10 °C. Globally, permafrost temperature increased by 0.29 ± 0.12 °C.

However, despite the great efforts by the GTN-P/IPA in managing qualified long-term permafrost observations at a global scale, the observation points are very scarce and clustered. For example, Biskaborn et al. (2015) pointed out that GTN-P permafrost boreholes and active layer measurement sites are clustered along transportation corridors in areas with developed infrastructure. They further demonstrated that the distribution of GTN-P sites is concentrated within zones where projected temperature rise is smaller while a much lower number of sites are located within Arctic areas where climate models project very large temperature increases.

There is currently no globally consistent and spatially continuous mapping of the ECV parameters permafrost temperature and active layer thickness. IPA has therefore recently established a permafrost mapping group (action group 'Overseeing the production of the next generation of IPA global permafrost mapping product and service'), which seeks to assess different permafrost mapping initiatives for the compilation of a new global database for permafrost properties. Permafrost_cci contributes to this IPA activity by providing satellite-driven permafrost datasets. The Permafrost_cci products are further expected to aid understanding of permafrost dynamics by satellite-observed land surface changes across large regions, in particular disturbances along latitudinal gradients as well as degradation associated with permafrost coastal processes.

The following sections provide a first assessment of the CRDPv0, v1 or v2 by the climate research group with respect to the so far identified applications.

Three user case studies are currently in process to cover a broad range of applications demonstrating the value and impact of CCI+ Permafrost products for different aspects of climate research. A utility assessment based on the PVIR is provided in addition.

3.2 Use Case Study 1 - Climate modelling

Models used for future projections of our climate have increased in complexity during the last years, going from General Circulation Models that mainly represented the atmosphere to fully coupled Earth System Models that try to represent all parts of the climate system, including biosphere, ocean, sea ice and the cryosphere. The focus of further developing those models is on a better representation of the processes relevant for the climate system, to allow better projections of possible futures.

The focus of our climate studies is on the Arctic, since it is one of the key areas of global warming. Here, we apply the Team Climate Model HIRHAM, which is a state-of-the-art atmospheric regional climate model (Christensen et al., 2007), for the circum-Arctic domain. The original land-surface-soil scheme of the model has been replaced by the advanced land model CLM4 (Community Land Model version 4) (Matthes et al., 2017) to improve descriptions of vegetation and soil processes, and especially to improve the representation of permafrost-related processes.

With this improved process understanding and representation in the model, we faced a new challenge of supplying the model with accurate boundary parameters, such as adequate soil stratigraphy information, distribution of organic matter and a good description of the vegetation. We used the CCI+ Landcover product to create vegetation maps as they are used by the model, converting the land cover classes into plant functional types (pfts), which can be interpreted as classes of plants with similar phenology. Those maps were used to replace existing maps which were based on MODIS data. In addition, the CCI+ Permafrost stratigraphy product was used to replace the existing mineral and organic soil maps based on the FAO soil map of the world.

In order to assess the impact of the boundary parameters for vegetation and soil in the coupled model HIRHAM-CLM on representation of the cryosphere and atmosphere, we conducted nine different model runs and evaluated them against in situ measurements and remote sensing based data products from

CCI+ Permafrost. The model was run from 1979-2019 with lower and lateral boundary forcing from the ERA5 reanalysis. A description of the differences in the model runs can be found in Table 1.

Table 1: Overview of the different experiment designs and naming convention for the model runs

	ctrl (pM_sFF)	ini2018	pE_sFF	pM_sFO	pM_sOF	pM_SOO	pE_sFO	pE_sOF	pE_sOO
vegetation	MODIS	MODIS	Landcover_cci	MODIS	MODIS	MODIS	Landcover_cci	Landcover_cci	Landcover_cci
mineral soil	FAO	FAO	FAO	FAO	Obu et al	Obu et al	FAO	Obu et al	Obu et al
organic soil	FAO	FAO	FAO	Obu et al	FAO	Obu et al	Obu et al	FAO	Obu et al
initialization	1979	2018	1979	1979	1979	1979	1979	1979	1979

In a first step, we made an assessment of cryosphere variables. CCI+ Permafrost provides mean annual ground temperature (MAGT) at 1m depth, which was average over the available time period (2003-2019) and compared to model output (see Figure 1). Comparison of the control run pM_sFF with the CCI+ Permafrost result shows overestimation of MAGT in high mountain and coastal areas of up to 6K, and an underestimation in western Eurasia and lowland regions of Siberia of up to -6K. Changing the initial state of the model (ini2018), the pft distribution (pE_sFF) and the mineral soil parameters (pM_sOF, pE_sOF) has only small impacts on the bias, the general structure remains the same. Changing the organic soil parameters however has a general warming impact on modelled MAGT. Existing warm biases are intensified, the cold biases over the Eurasian Arctic disappear, the cold strong cold biases over Siberia become small warm biases.

In a second step, we examined atmosphere conditions. For evaluation with air temperature data from more than 300 WMO stations around the Arctic are used. We looked into monthly mean temperature averaged over 1979-2019. Biases and root mean square errors are shown in Table 1. All model runs with no changes of organic matter have similar root mean square errors averaged over the year as the reference run. On the contrary, runs with changed organic matter have improved root mean square errors in the annual average, particularly the summer and autumn months are improved.

In summary, changing boundary parameters for land has significantly impacted soil temperatures in our model runs. Using all boundary parameters derived from CCI Landcover and CCI Permafrost improved not only the representation of soil temperature but also the representation of air temperature.

Table 2 : Comparison of climatological monthly mean 2m air temperature from model runs and WMO meteorological station data.

	ref	ini2018	pM_sOO	pM_sFO	pM_sOF	pE_sFF	pE_sOO	pE_sFO	pE_sOF
	bias	bias	bias	bias	bias	bias	bias	bias	bias
jan	-0,6	-0,6	-0,5	-0,5	-0,6	-0,7	-0,6	-0,5	-0,7
feb	-0,9	-1,0	-0,9	-0,9	-1,0	-1,1	-1,0	-1,0	-1,1
mar	-1,9	-1,8	-1,8	-1,7	-1,9	-1,9	-1,9	-1,9	-2,0
apr	-2,3	-2,3	-2,2	-2,2	-2,4	-2,3	-2,3	-2,3	-2,3
may	-1,9	-1,9	-1,9	-1,9	-1,9	-1,9	-1,8	-1,9	-1,9
jun	-1,7	-1,7	-1,7	-1,7	-1,7	-1,7	-1,6	-1,7	-1,6
jul	-2,2	-2,2	-2,0	-2,2	-2,1	-2,1	-2,0	-2,1	-2,0
aug	-2,1	-2,1	-1,9	-1,9	-2,1	-2,0	-1,8	-1,9	-2,0
sep	-1,8	-1,8	-1,7	-1,6	-1,9	-1,8	-1,6	-1,6	-1,8
oct	-1,9	-2,0	-1,8	-1,7	-2,0	-1,9	-1,7	-1,6	-1,9
nov	-1,4	-1,3	-1,2	-1,2	-1,3	-1,4	-1,2	-1,2	-1,4
dec	-0,8	-0,8	-0,7	-0,7	-0,9	-0,9	-0,9	-0,8	-0,9
	-1,63	-1,63	-1,51	-1,51	-1,64	-1,65	-1,53	-1,53	-1,64

ref	ini2018	pM_sOO	pM_sFO	pM_sOF	pE_sFF	pE_sOO	pE_sFO	pE_sOF
rmse	rmse	rmse	rmse	rmse	rmse	rmse	rmse	rmse
2,6	2,6	2,6	2,7	2,6	2,7	2,7	2,7	2,7
2,6	2,7	2,7	2,7	2,7	2,8	2,8	2,8	2,8
3,2	3,2	3,1	3,1	3,2	3,3	3,2	3,2	3,3
3,6	3,5	3,4	3,5	3,6	3,5	3,5	3,5	3,5
2,8	2,8	2,7	2,8	2,8	2,7	2,7	2,7	2,8
2,2	2,2	2,2	2,3	2,2	2,2	2,2	2,3	2,2
2,6	2,6	2,5	2,6	2,5	2,5	2,5	2,6	2,4
2,4	2,4	2,2	2,3	2,4	2,4	2,2	2,2	2,3
2,3	2,3	2,1	2,0	2,3	2,2	2,0	2,0	2,3
2,8	2,8	2,6	2,5	2,8	2,8	2,5	2,5	2,8
2,6	2,5	2,5	2,5	2,5	2,6	2,5	2,5	2,6
2,7	2,7	2,7	2,7	2,7	2,7	2,8	2,7	2,7
2,69	2,69	2,61	2,62	2,69	2,70	2,63	2,64	2,70

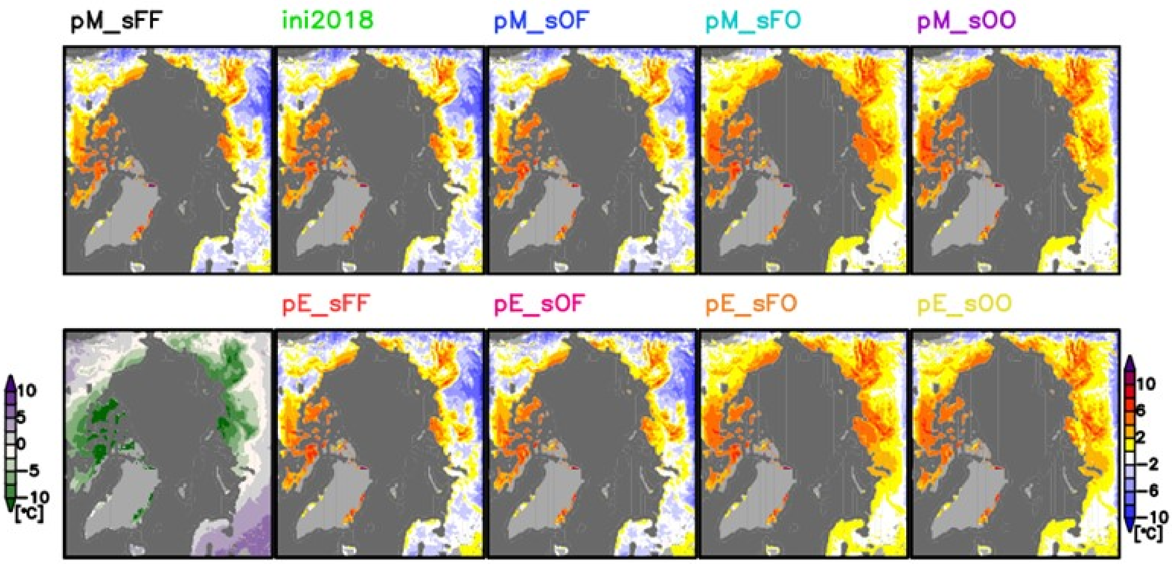

Figure 1: Mean annual ground temperature at 1m depth, averaged over 2003-2019, from CCI+ Permafrost product (lower left panel) and difference to model runs (model run minus CCI+Permafrost).

3.3 Use Case Study 2 -ALT, PFR and ground temperature trends: comparison to landcover trends

The Science use case 2 in Permafrost_cci focuses on the cross-analysis of the existing ESA GlobPermafrost Hot Spot Regions of Permafrost Change (HRPC) product with output from the Permafrost_cci transient permafrost model. The HRPC contains information on Landsat-based trends of landscape disturbances, which may trigger changes in the ground thermal regime or become enhanced by regional to local changes in ground thermal regime.

We hypothesize that climatic fluctuations directly impact permafrost properties and ground thermal regime as measured by active layer thickness (ALT) or permafrost/ground temperature. This in turn will likely impact the initiation and enhancement of permafrost region disturbances (PRD).

Based on this hypothesis we spatially compared the HRPC data products (Nitze et al., 2018 a,b) with the dynamic annual (1997-2018) ALT and PFR (permafrost probability) as well as static permafrost temperature Permafrost CCI+ data products (Obu et al, 2018) for all four core transects of the HRPC data analysis in western Siberia (T1), eastern Siberia (T2), Alaska (T3), and eastern Canada (T4).

Lake drainage - ground temperature relationship

A first cross-analysis between current Permafrost_cci products and GlobPermafrost HRPC disturbance trends focused on the analysis of the spatial relationship between lake drainage and mean annual ground temperature. Lake changes were quantified using trends of multispectral indices of Landsat-time series data from 1999 through 2014 (Nitze et al., 2017, 2018). This includes net lake changes of each individual lake (<1ha) within the transects, as well as the gross increase and decrease (individual fractions of lake area gain and loss). Furthermore, we calculated lake shore change rates in cm per year for each individual lake (n > 600,000).

Lakes in permafrost often exhibit a dynamic behaviour, where lakes often expand over time and ultimately drain once they reach a drainage gradient or permafrost destabilizes. Lake drainage can occur in different magnitudes, where lakes can drain completely or only partially.

Figure 2 shows the relation between net lake area loss of shrinking lakes (negative net lake change) from the HRPC lake change datasets (Nitze et al., 2018b) for all 4 analyzed continental scale permafrost transects. It reveals distinct clusters of lake area loss intensity and mean annual ground-temperature MAGT distributions. All sites show a bimodal distribution of lake area loss, but with different magnitude. The first cluster is typically located at <20 % lake area loss (net change), which is caused by subtle lake fluctuations, data uncertainty, partial lake drainage or a combination of these factors. Lakes with a lake area increase were kept from the analysis. This cluster is the most dominant in T4 (Eastern Canada), which is characterized by mostly stable lake areas across the transect region and thus the permafrost temperature gradient. The second cluster is typically close to 100%, which translates to complete lake drainage. This second cluster is more common in Transects T1-T3, which are more dominated by frozen ice-rich sediments rather than glacially-carved bedrock like T4. The relation of these drainage clusters to MAGT is diverse among the different transects. While T2 is characterized by cold MAGT of predominantly <-4 °C, complete lake drainage events clustered at around -6 °C. In T1 and T3, which have very strong lake dynamics (Nitze et al., 2018a), the complete drainage cluster is close to 0 °C, which may indicate the influence of landscape-scale permafrost degradation and widespread surface permafrost loss in the affected regions. However, regional conditions and differences should be considered and more detailed local to regional-scale analysis will reveal further links between ground temperature, other environmental factors, and the dynamics of permafrost region disturbances such as lake drainages.

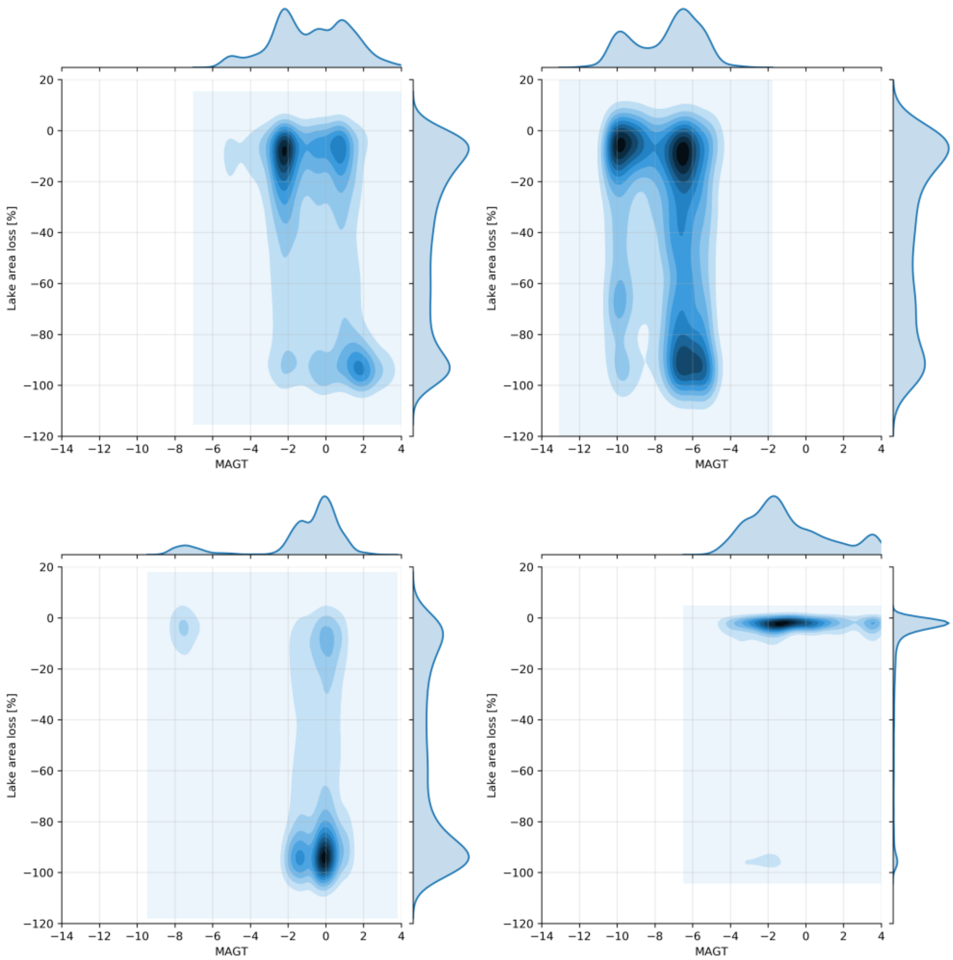

Figure 2: 2D density plots of lake area loss % (per lake) vs. MAGT. Darker colors represent a higher density and thus more lake drainage events. Upper left: T1 Western Siberia; upper right: T2 Eastern Siberia; lower left: T3 Alaska; lower right: T4 Eastern Canada.

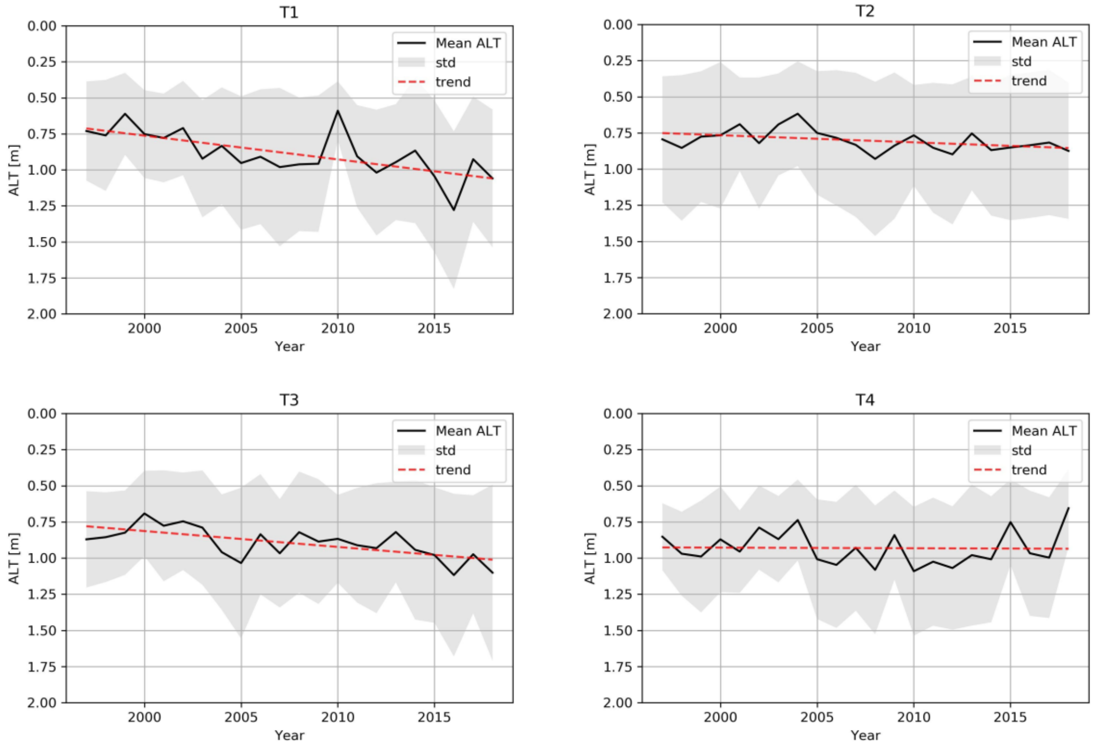

Figure 3. Comparison of Active Layer Thickness dynamics (in meter) in different HRPC Transects (T1: Western Siberia, T2: Eastern Siberia, T3: Alaska, T4: Eastern Canada) derived from annual ALT datasets (1997-2018).

Active layer thickness dynamics

The active layer trends show clear differences between the different transect regions (Figure 3). Transects T1 and T3 show the largest increase in mean ALT, which correlates with the observed lake drainage dynamics. Larger regions within both transects were particularly affected by lake drainage within the past two decades (Nitze et al., 2017, 2018, 2020). Transect T2 was much less affected by ALT deepening, while Transect T4 has a flat trend, although with strong annual fluctuation.

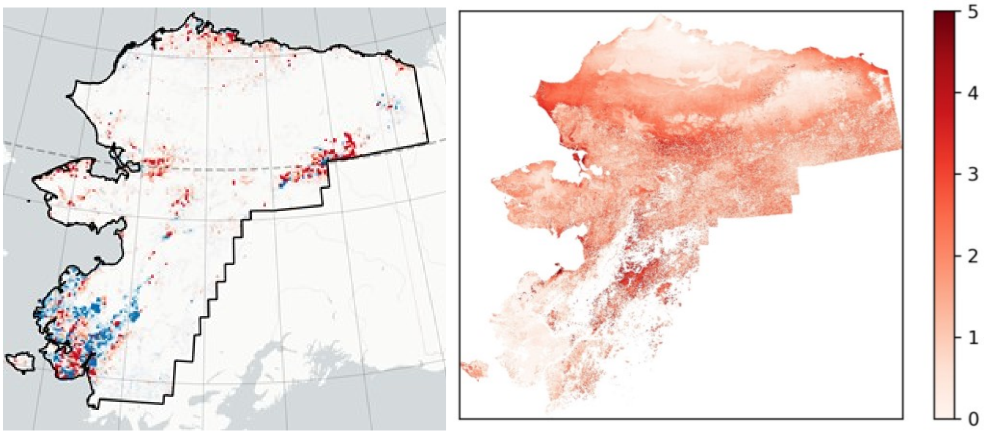

Figure 4: Spatial comparison of (left) Lake area change (1999-2014) from HRPC Datasets and (right) increase in Active Layer Thickness (ALT) trends in % from annual CCI ALT dataset in T3 Alaska.

Wildfire - ALT interactions

Wildfires are a widespread disturbance in the boreal, mostly semi-arid continental permafrost regions such as Central Yakutia, interior Alaska or NW Canada. Two of these regions are located within the HRPC transects T2 and T3. We analyzed the ALT trajectories from 1999 until 2018 within burned areas, non-burned areas and individual fire scars. For this purpose we calculated the mean and standard deviations of annual ALT within the burn scars. Furthermore we applied a linear model to compare the change (slope) in mean ALT and its standard deviation for each region and burn status.

Table 3: Change in mean and standard deviation of Active Layer Thickness in burned and non-burned areas across all 4 transects.

	Fire		No Fire	
Region	*Mean*	*Std*	*Mean*	*Std*
T1	+40.10	+102.23	+49.11	+47.44
T2	+15.45	+21.66	+13.59	+10.11
T3	+30.05	+95.73	+29.74	+59.37
T4	+30.95	+56.63	+0.86	+34.33

Individual Fires

On an individual burn scar level we can directly identify the impact of wildfires. Figure 5 shows the mean (line) and standard deviation (shading) of ALT for the Anaktuvuk River fire scar area from 1999 through 2018. The Anaktuvuk tundra fire in northern Alaska (Jones et al, 2009) burned around 1000 km² (100,000 ha) tundra, partially underlain by ice-rich permafrost, in late summer 2007. Before the large fire in 2007, the mean ALT fluctuated rather strongly (mean ALT 0.53-0.75), depending on annual weather conditions. However, The variance within the analysed site was very low which indicates a rather homogeneous ALT. After the intense tundra fire mean ALT increased to deeper depths (0.7-0.8 m). At the same time the variance of ALT increased markedly within the burned region.

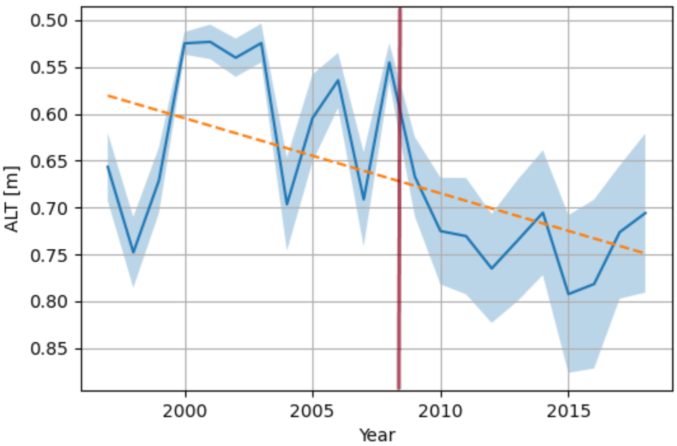

Figure 5: Mean (line), standard deviation (shading) and trend of mean (orange dashed line) of modelled active layer thickness (ALT) within the Anaktuvuk firescar in northern Alaska. Burn date (2007) indicated with a red line.

In all sites, ALT was larger for burned sites than for non-burned sites, which can be expected as wildfires predominantly occur in warmer, forested boreal sites. However, the trajectories of ALT exhibit a different behaviour. In all transects T1-T4, mean ALT increased within burned areas (+15-40%), but also in non-burned areas (+14-49%), except T4 (+1%), with similar magnitudes between burned and non-burned areas (Table 3) . In comparison, variance of ALT increased in burned sites within all transects increased much stronger than in non-burned areas, even (almost) doubling in standard deviation.
Although the impact of wildfire on ALT seems to be much stronger in T4, the impact on ground stability may be much weaker than in the other regions, due to primarily underlying bedrock. We hypothesize a much stronger effect of increasing ALT in e.g. ice-rich permafrost in Alaska (T3) or eastern Siberia (T2). Particularly increasing variance within burned areas, with locally strong increase in ALT, may result in triggering further permafrost disturbances. However, more detailed analysis will be conducted to verify/falsify this hypothesis.

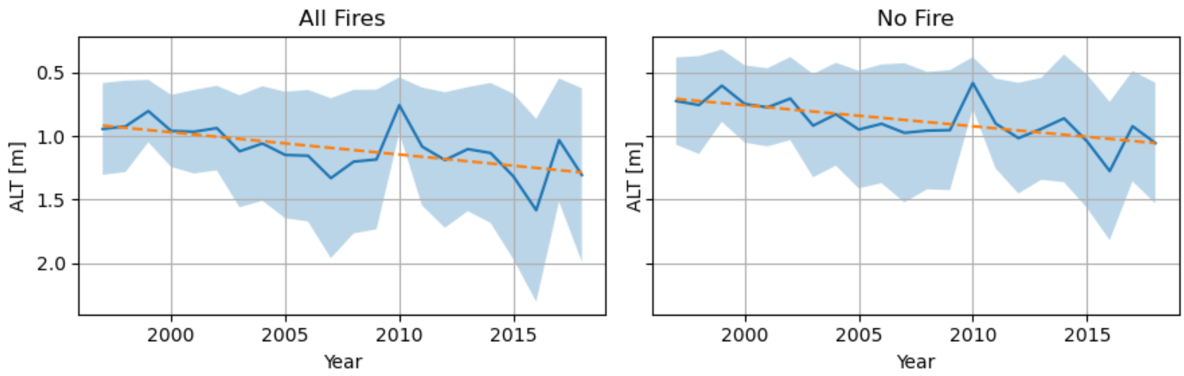

Figure 6: Mean (line), standard deviation (shading) and trend of mean (orange dashed line) of modelled active layer thickness (ALT) in burned and unburned regions in Transect T1 Western Siberia.

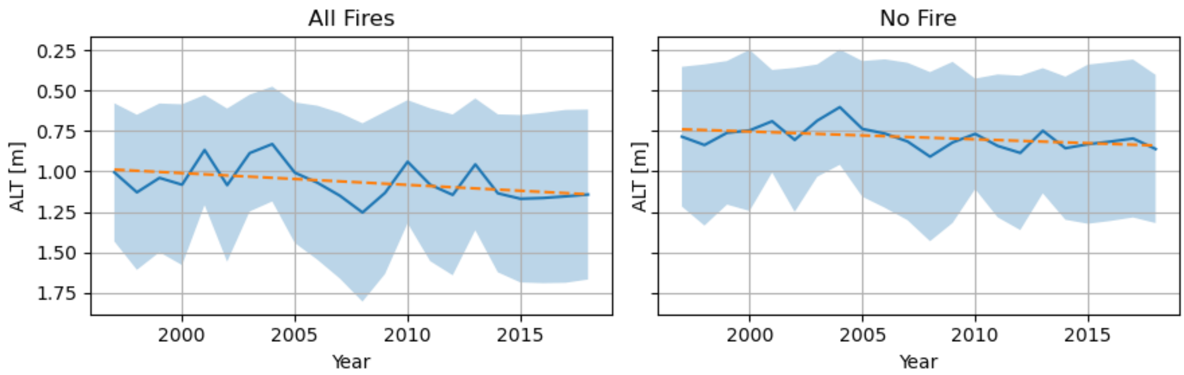

Figure 7: Mean (line), standard deviation (shading) and trend of mean (orange dashed line) of modelled active layer thickness (ALT) in burned and unburned regions in Transect T2 Eastern Siberia.

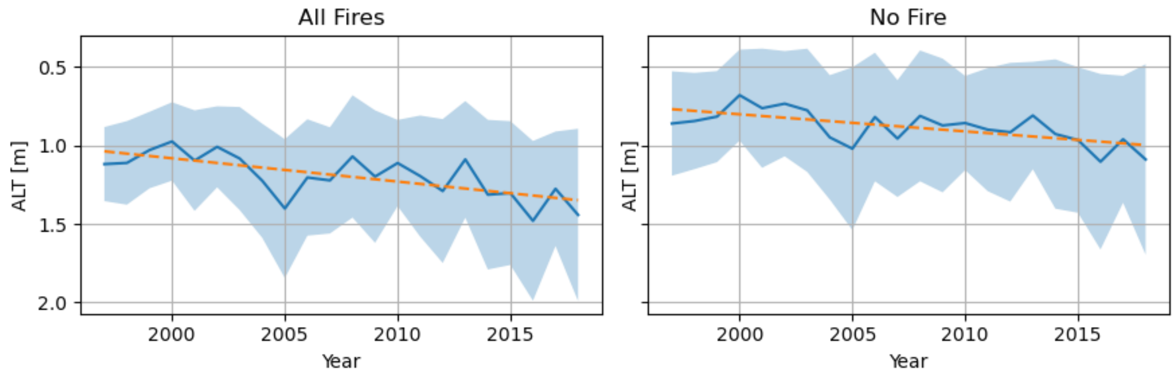

Figure 8: Mean (line), standard deviation (shading) and trend of mean (orange dashed line) of modelled active layer thickness (ALT) in burned and unburned regions in Transect T3 Alaska.

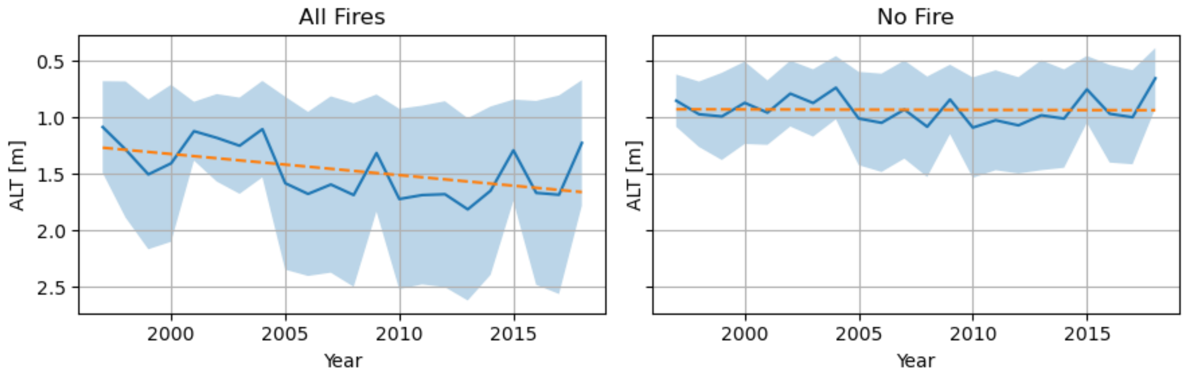

Figure 9: Mean (line), standard deviation (shading) and trend of mean (orange dashed line) of modelled active layer thickness (ALT) in burned and unburned regions in Transect T4 Eastern Canada.

3.4 Use Case Study 3 - Ground temperature trends: comparison to coastal erosion

The overall strategy of the HORIZON2020 Nunataryuk project (2017-2022) is to bring together high-ranking European and international specialists of the Arctic coast, including natural scientists and the key European socio-economic science groups, to address challenges in a transdisciplinary way. The project is user-driven, directly addressing the concerns of local and global stakeholders with regards to permafrost thaw in coastal areas of the Arctic. Permafrost thaw is the core focus of Nunataryuk and is also used as the common thread for consultations with community representatives and other stakeholders at the local and global level. Time series as developed by Permafrost_cci are therefore of high value to the project. They are utilized as part of scenario building workshops, stakeholder communication as well as to interpret natural science results of the project. The latter overlaps with case study 3. CRDPv0 (2002-2017 records) already provided valuable information (Bartsch et al. 2020). In order to assess SAR applicability for coastal erosion quantification, data acquired at three different wavelengths (X-, C-, L-band; TerraSAR-X, Sentinel-1, ALOS PALSAR 1/2) have been investigated. Four regions which feature high erosion rates have been selected. All three wavelengths have been investigated for Kay Point (Canadian Beaufort Sea Coast). C- and L-band have been studied at all sites, including Herschel Island (Canadian Beaufort Sea Coast), Varandai (Barents Sea Coast, Russia), and Bykovsky Peninsula (Laptev Sea coast, Russia). Erosion rates have been derived for a one-year period (2017-2018) and in the case of L-band also over 11 years (2007-2018). The Landsat trend product (see case study 2) has been in addition assessed for long-term trend retrieval. Derived retreat rates agree among the datasources /SAR and Landsat trends) and with rates available from other data sources. The derived rates suggest an increase of erosion at all four sites in recent years (Figure 10), but uncertainties are also high. However, CRDPv0 ground temperatures at 2 m depth have also been increasing at all these sites between 2003-2017.

	Rate from GlobPermafrost trend product 1999-2014	Rate from L-band SAR 2007-2018	Previously published rates
Varandai (c)	n.a.	-5.41 ± 2.64	-1.8 (1951-2013) [1]
Herschel (B)	-4.19 ± 2.8	-7.02 ± 2.65	-6.8 (2012-2013) [2]
Kay Point (B)	-3.94 ± 1.4	-5.90 ± 0.41	-1.7 (1990-2011) [3]
Bykosvky (D)	-5.83 ± 2.8	-4.81 ± 1.37	-1 - -2 (1951-2006) [4]

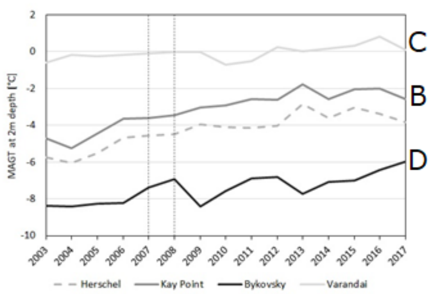

(1) Sinistyn et al. 2019, (2) Obu et al. 2016, (3) Irrgang et al. 2017, (4) Lantuit et al. 2011

Figure 10: Erosion rate retrieval summary from Bartsch et al. (2020). Most sites show increased recent rates (left) as well as increasing ground temperatures (right, source CRDPv0).

3.5 Further documented use

Permafrost_cci active layer thickness

- Brouillette, M. (2021). How microbes in permafrost could trigger a massive carbon bomb. Genomics studies are helping to reveal how bacteria and archaea influence one of Earth's largest carbon stores as it begins to thaw. News Feature. *Nature*, *591*(7850), 360–362. https://doi.org/10.1038/d41586-021-00659-y
- Tamm., J. (2021): Remote-sensing based assessment of post-fire changes in land surface temperature in Arctic-Boreal permafrost regions. Master Thesis, University of Potsdam. 74pp.

GlobPermafrost Permafrost extent use examples

- Ramage, J., Jungsberg, L., Wang, S., Westermann, S., Lantuit, H. & Heleniak, T. (2021), 'Population living on permafrost in the Arctic',Population and Environment.URL:https://doi.org/10.1007/s11111-020-00370-6
- Julian Murton, Periglacial Processes and Deposits, Editor(s): David Alderton, Scott A. Elias, Encyclopedia of Geology (Second Edition), Academic Press, 2021, Pages 857-875, ISBN 9780081029091, https://doi.org/10.1016/B978-0-12-409548-9.11925-6.
- Kåresdotter, E., Destouni, G., Ghajarnia, N., Hugelius, G., & Kalantari, Z. (2021). Mapping the vulnerability of Arctic wetlands to global warming. Earth's Future, 9, e2020EF001858. https://doi.org/10.1029/2020EF001858
- Lapierre Poulin, F., Fortier, D., & Berteaux, D. (2021). Low vulnerability of Arctic fox dens to climate change-related geohazards on Bylot Island, Nunavut, Canada. *Arctic Science*, 1–16. https://doi.org/10.1139/as-2019-0007

- Webb, E. E., Loranty, M. M., & Lichstein, J. W. (2021). Surface water, vegetation, and fire as drivers of the terrestrial Arctic-boreal albedo feedback. Environmental Research Letters, 16(8), 084046. https://doi.org/10.1088/1748-9326/ac14ea
- Horizon2020 project Nunataryuk (GRID Arendal): Foldable map of permafrost around the world https://www.grida.no/news/13
- Ardelean, F., Onaca, A., Chețan, M.-A., Dornik, A., Georgievski, G., Hagemann, S., Timofte, F., & Berzescu, O. (2020). Assessment of Spatio-Temporal Landscape Changes from VHR Images in Three Different Permafrost Areas in the Western Russian Arctic. Remote Sensing, 12(23), 3999. https://doi.org/10.3390/rs12233999

Climate modelling:

- Burke, E.J., Zhang, Y., Krinner, G. (2020): Evaluating permafrost physics in the Coupled Model Intercomparison Project 6 (CMIP6) models and their sensitivity to climate change, The Cryosphere, 14, 3155–3174, 2020, https://doi.org/10.5194/tc-14-3155-2020

3.6 Permafrost_cci utility based on evaluation results

This science case study is the utility assessment of the Permafrost_cci ECV products. The independent validation is carried out with strong support of the user community, with in situ measurements characterised by community-wide management best practises with open data access and a collaborative user environment within an international framework: WMO and GCOS delegated the global monitoring of the ECV Permafrost to the Global Terrestrial Network for Permafrost (GTN-P) that is managed by the International Permafrost Association (IPA). GTN-P/IPA established the Thermal State of Permafrost Monitoring (TSP) for permafrost temperature and the Circumpolar Active Layer Monitoring program (CALM) for active layer thickness monitoring. The national-wide Russian meteorological monitoring network ROSHYDROMET additionally provides long-term ground temperature records close to meteorological stations. GTN-P and ROSHYDROMET time series and data collections from additional networks provide reference data sets, however no easy-to use or readily available time-series depth data that are data-fit for validation. We assembled standardised reference data from 1997 to 2019 spanning permafrost regions from Scandinavia to higher latitude permafrost and all altitude ranges from lowland to mountain permafrost across a wide range of latitudes, altitudes, climate zones, land cover, and lithologies.
Permafrost_cci CRDPv2 provides 1 km pixel resolution ECV products on mean annual ground temperature (MAGT) at discrete ground depths (product name GTD), Active Layer Thickness (product name ALT) and Permafrost Fraction (product name PFR). Permafrost_cci GTD, ALT and PFR time series from 1997 to 2019 come with an annual resolution. The match-ups were executed using a pixel-based approach. Permafrost_cci GTD is provided in 0,1,2,5, and 10 m depth and depth-interpolated to fit the depths of the extensive in situ data set. The match-up data is standardized but still contains a large variability of match-up pairs in time, region, and reference depths.

Permafrost_cci GTD match-up evaluation between simulated Permafrost_cci and in situ measurements showed the following performance characteristics: Overall, the simulation dataset with n = 14,107 match-up pairs in time and depth from 354 sites had a median MAGT bias of -1.12 °C. 4,672 Match-up pairs from 234 in situ measurements sites confined to MAGT < 1°C and thus from reliable permafrost sites showed a much better performance with a median bias of 0.2°C compared to the full dataset including in situ MAGT >= 1°C along the southern boundary of the discontinuous and sporadic permafrost zone. A relatively large proportion of residuals >95% quantile were located across Alaska, specifically in the boreal regions.

As a consequence of the cold bias in the warm temperature range, the binary match-up of 'permafrost' versus 'no permafrost' for Permafrost_cci PFR versus in situ MAGT ranges shows that PFR in the grid cell is overestimated compared to in situ-derived 'no permafrost' and MAGT ≤0.5 °C. Permafrost_cci PFR in the grid cell >0% occurs together with a wide range of 'warm' in situ MAGT >0 °C. Overall, the majority of match-up pairs (69.9%) were in agreement between the in-situ proxy and the Permafrost_cci simulation. Notably, the 100% and the 0% PFR had high percentage of agreement, with 97.04% and 91.03% match respectively. Geographically, most mismatches were located in the Eurasian southern boundary of the permafrost extent. The high agreement in the 100% and 0% Permafrost_cci PFR groups was stable across years. In general, the agreement in the <100% and >0% groups increased towards the end of the time series (2019).

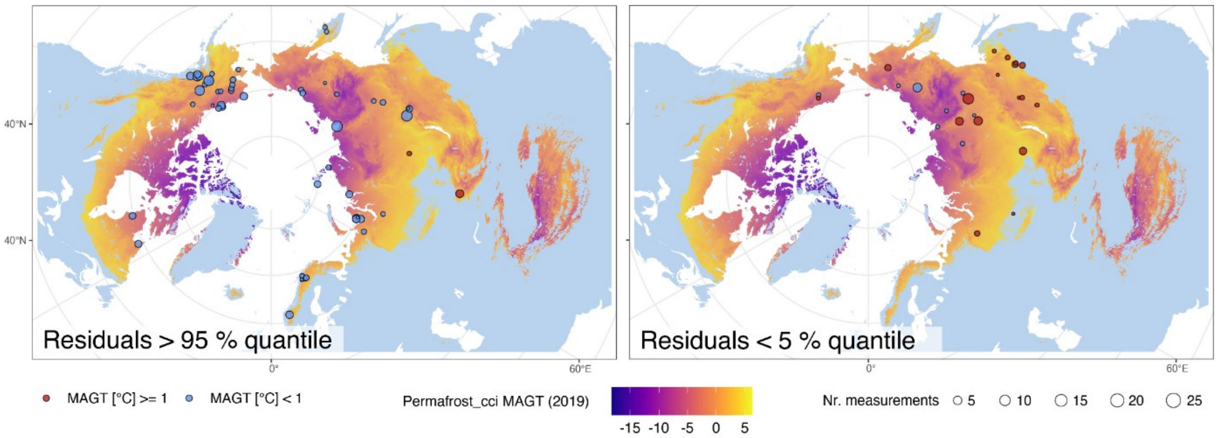

Figure 13 Location of residuals > 95% quantile (left) and < 5% quantile (right). Color of circles represents the temperature subset and size of the circle represents the number of samples at the particular location.

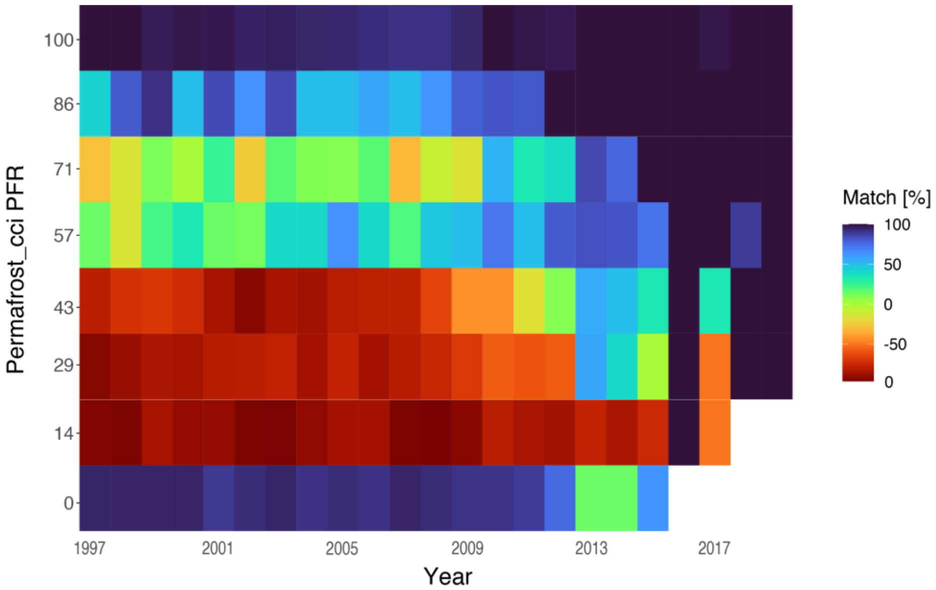

Figure 14: Match-up summary of Permafrost_cci PFR with in-situ MAGT and ALT dataset over years.

PERMOS investigations in the Swiss Alps showed in contrast a warm model bias of Permafrost_cci MAGT. Therefore, the extent of permafrost simulated by Permafrost_cci PFR was too restrictive. In the Swiss Alps, the lower limit of permafrost is usually found around 2600 m a.s.l. ±200 m whereas for Permafrost_cci PFR the lower limit is found around 3000 m a.s.l.. Furthermore, the vast majority of inventoried ESA GlobPermafrost slope movement products are located outside of the simulated Permafrost_cci permafrost extent area and only six amongst the 12 PERMOS permafrost borehole sites were located within the simulated Permafrost_cci PFR permafrost extent area. Positively, although the absolute values are significantly different, both, the measured and the simulated MAGT, show the warming trend over the period 1997-2019.

For the Permafrost_cci ALT match-up analyses, we were restrictive with focus on high-latitude to mid-latitude permafrost regions related to the Permafrost_cci model parameterization, thereby excluding all sites in Mongolia, Central Asia, on the Tibetan Plateau (China) due to their different snow and subground regimes. Permafrost_cci ALT performance for in situ ALT with match-up pairs from China and Mongolia excluded is characterised by a median bias of 3 cm (95% CI: -11 to 123 cm). Differences in trends over time between Permafrost_cci and in-situ measurements are larger compared to the MAGT product: only the majority of 58% of Permafrost_cci ALT trends over time match the in-situ trends, however, the ALT match-up sample size is also considerably smaller. Large residuals >1 m are obvious in the warmer permafrost zones in forested regions of Alaska, Canada and Central Siberia (Permafrost_cci negative bias with simulated shallow ALT versus deep in-situ ALT). Also, residuals >1.5 m cluster in Svalbard (Permafrost_cci positive bias with simulated deep ALT versus shallow in-situ ALT).

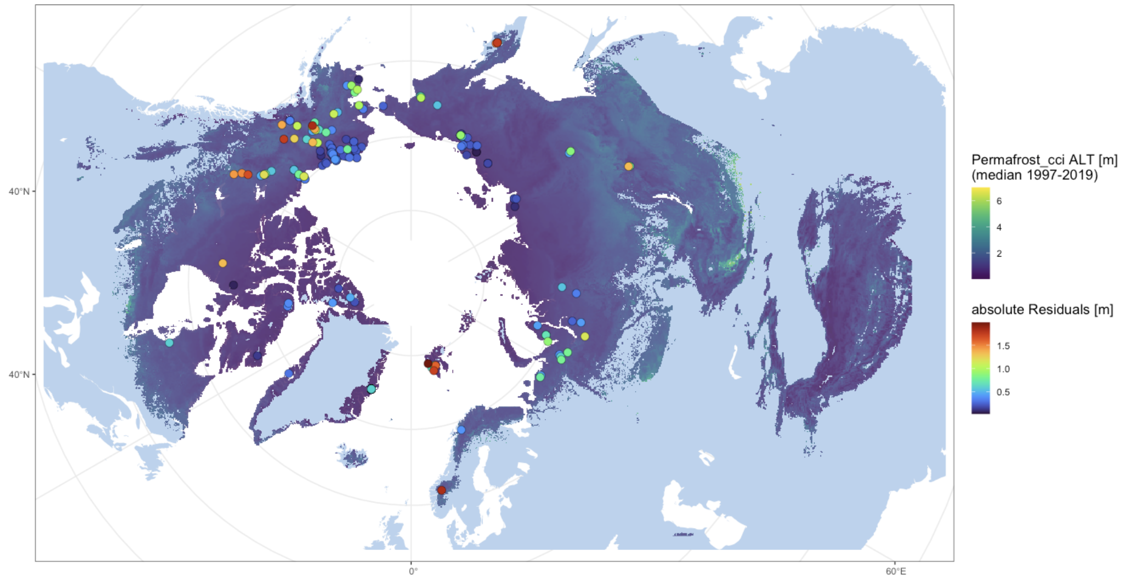

Figure 15. Spatial distribution of maximum residual per site from Permafrost_cci ALT and in situ ALT match-up over active layer thickness depths in cm.

In summary, the Permafrost_cci permafrost temperature type (that we defined as GTD < 1°C) showed good performance across the Northern hemisphere, with a median bias of 0.2°C for all depths. Users of Permafrost_cci GTD products should however consider, that Permafrost_cci GTD> 1°C of the discontinuous, sporadic and non-permafrost zones is characterized by a cold median MAGT bias of -1.47 °C. This leads in turn to too shallow simulated Permafost_cci active layer thickness in the permafrost continuous zones around the lower 60° Latitudes and an overestimation of the areal extent of permafrost (for Permafrost_cci Permafrost FRraction PFR < 50 %) at the southern boundaries of Permafrost in discontinuous, and sporadic permafrost regions along the southern boundary of permafrost in Eurasia. PERMOS investigations in the Swiss Alps showed in contrast a warm model bias of Permafrost_cci MAGT ranging from +1.22°C at the surface to +1.81°C at 10 m depth with the vast majority of inventoried ESA GlobPermafrost slope movement products located outside of the simulated Permafrost_cci permafrost extent area (Permafrost_cci PFR).

We thus consider Permafrost_cci GTD and PFR products for the Northern hemisphere to be most reliable in the permafrost temperature range with GTD < 1°C and in PFR >50% as well as PFR <14% is reliable as non-permafrost. Further integrating data on stratigraphy, ground ice, vegetation and more will in turn lead to process understanding of linkages of vegetation, hydrology, lithology, topography, climate and permafrost properties. Vincent et al., (2017) formulated the '3-layer Permafrost Earth System approach': The two geo/cryosphere layers are the active layer and permafrost. The 3rd layer, the buffer layer, consists of the biosphere (vegetation from polar desert to tundra to boreal) and hydrology (e.g., snow) also including infrastructure. We plan to complement the temperature and active layer reference data with contextual data on the two geo/cryosphere layers (active layer and permafrost): ground stratigraphy and lithology, ground ice content, and ground texture. Contextual data are also provided for the 3rd layer, the buffer layer, in the form of information on vegetation, surface habitus, and infrastructure.

4 PROGRESS IN REGARD TO USER REQUIREMENTS

4.1 Algorithm selection

The process of the algorithm selection as detailed in the User Requirements Document (URD) [RD-4] has been driven by the requirements of the climate research community. The user community deemed the selected algorithm as appropriate for their applications.

4.2 Product specification

In Table 1, we specify user requirements from the URD [RD-4] and added for each year a column to mark the respective status of achievement. We aimed to complete as many requirements as possible, which are marked in green.

Table 4: Summary of user requirements. Background (BG) means that this is a continuous activity, production (P), and dissemination (D) means that the related requirement has to be considered during production, and dissemination, respectively. Parameters are Permafrost Extent (PE), Ground Temperature (GT) and Active Layer Thickness (ALT). The last column indicates the achievement status for the third project year (Y3=year 3; red: not started, yellow: ongoing, green: completed).

ID	Parameter	Requirements	Source	Type	Y3
URQ_01	PE/GT/ALT	higher spatial resolution than a map scale of 1:10,000,000	IPA Mapping group report	BG	
URQ_02	PE/GT/ALT	data need to be related to a time stamp	IPA Mapping group report	P	
URQ_03	PE/GT/ALT	form of delivery for maps and data need to be flexible	IPA Mapping group report	D	
URQ_04	PE/GT/ALT	high data quality	IPA Mapping group report	BG	
URQ_05	PE/GT/ALT	benchmark dataset needs to be developed	IPA Mapping group report, GlobPermafrost/IPA mapping group workshop	P	
URQ_06	PE/GT/ALT	evaluation through community	GlobPermafrost/IPA mapping group workshop	P	
URQ_07	PE/GT/ALT	terminology for modelling output 'potential'	GlobPermafrost/IPA mapping group workshop	D	
URQ_08	GT/ALT	depth of active layer, permafrost temperature in K and seasonal soil freeze/thaw needs to be addressed	GCOS	BG	
URQ_09	PE	Threshold: uncertainty 10-25%, hor. res. 10-100 km, temp. res. 3-5 days, timeliness 5-6 days;	OSCAR	BG	

		breakthrough uncertainty 7-8.5%, hor. res. 0.85 - 1 km, temp. res. 14-36 hours, timeliness 14-36 h			
URQ_10	PE/GT/ALT	Distribution as NetCDF	CMUG	D	
URQ_11	PE/GT/ALT	Development of a new ground stratigraphy product for the permafrost domain	GlobPermafrost survey	P/D	
URQ_12	GT	Threshold: pan-arctic, yearly, last decade, 10km, RMSE<2.5°C,	Permafrost_cci survey	BG	
		Target, global, monthly, 1979-present, 1km, subgrid variability, RMSE < 0.5°C			
URQ_13	ALT	Threshold: pan-arctic, yearly, last decade, 10km, RMSE<25cm,	Permafrost_cci survey	BG	
		Target, global, monthly, 1979-present, 1km, subgrid variability, RMSE<10cm			

5 PUBLICATIONS

5.1 Publications list

Published

Ardelean, F.; Onaca, A.; Chețan, M.-A.; Dornik, A.; Georgievski, G.; Hagemann, S.; Timofte, F.; Berzescu, O. (2020). Assessment of Spatio-Temporal Landscape Changes from VHR Images in Three Different Permafrost Areas in the Western Russian Arctic. Remote Sensing. 12(23), 3999. https://doi.org/10.3390/rs12233999

Bartsch, A., Ley, S., Nitze, I., Pointner, G., & Vieira, G. (2020). Feasibility study for the application of Synthetic Aperture Radar for coastal erosion rate quantification across the Arctic. Frontiers in Environmental Science, 8(143). https://doi.org/10.3389/fenvs.2020.00143

A. Bartsch, G. Pointner, H. Bergstedt, B. Widhalm, A. Wendleder, A. Roth (2021). Utility of polarizations available from Sentinel- 1 for tundra mapping. IGARSS 2021 proceedings.

Bergstedt, H., Bartsch, A., Neureiter, A., Höfler, A., Widhalm, B., Pepin, N., and Hjort, J. (2020). Deriving a Frozen Area Fraction From Metop ASCAT Backscatter Based on Sentinel-1. IEEE Transactions on Geoscience and Remote Sensing, Volume: 58, Issue: 9. https://doi.org/10.1109/TGRS.2020.2967364

Bergstedt, H., Bartsch, A., Duguay, C. R., & Jones, B. M. (2020). Influence of surface water on coarse resolution C-band backscatter: Implications for freeze/thaw retrieval from scatterometer data. Remote Sensing of Environment, 247, 111911. https://doi.org/10.1016/j.rse.2020.111911

M. Brouillette: How microbes in permafrost could trigger a massive carbon bomb. Nature, 591, 360-362 (2021) on 17 March 2021. https://www.nature.com/articles/d41586-021-00659-y

Biskaborn, B. K.; Smith, S. L.; Noetzli, J.; Matthes, H.; Vieira, G.; Streletskiy, D. A.; Schoeneich, P.; Romanovsky, V. E.; Lewkowicz, A. G.; Abramov, A.; Allard, M.; Boike, J.; Cable, W. L.; Christiansen, H. H.; Delaloye, R.; Diekmann, B.; Drozdov, D.; Etzelmüller, B.; Grosse, G.; Guglielmin, M.; Ingeman-Nielsen, T.; Isaksen, K.; Ishikawa, M.; Johansson, M.; Johannsson, H.; Joo, A.; Kaverin, D.; Kholodov, A.; Konstantinov, P.; Kröger, T.; Lambiel, C.; Lanckman, J.-P.; Luo, D.; Malkova, G.; Meiklejohn, I.; Moskalenko, N.; Oliva, M.; Phillips, M.; Ramos, M.; Sannel, A. B. K.; Sergeev, D.; Seybold, C.; Skryabin, P.; Vasiliev, A.; Wu, Q.; Yoshikawa, K.; Zheleznyak, M., Lantuit, H. (2019): Permafrost is warming at a global scale. Nature Communications, 10, 264. https://doi.org/10.1038/s41467-018-08240-4

Biskaborn, B. K., Lanckman, J.-P., Lantuit, H., Elger, K., Streletskiy, D. A., Cable, W. L., and Romanovsky, V. E. (2015): The new database of the Global Terrestrial Network for Permafrost (GTN-P). Earth Syst. Sci. Data, 7, 245–259. https://doi.org/10.5194/essd-7-245-2015

Burke, E. J., Zhang, Y., & Krinner, G. (2020). Evaluating permafrost physics in the Coupled Model Intercomparison Project 6 (CMIP6) models and their sensitivity to climate change. The Cryosphere, 14(9), 3155–3174. https://doi.org/10.5194/tc-14-3155-2020

Jones, B. M. , Arp, C. D. , Grosse, G. , Nitze, I. , Lara, M. J. , Whitman, M. S. , Farquharson, L. M. , Kanevskiy, M. , Parsekian, A. D. , Breen, A. L. , Ohara, N. , Rangel, R. C. and Hinkel, K. M. (2020): Identifying historical and future potential lake drainage events on the western Arctic coastal plain of Alaska. Permafrost and Periglacial Processes, 31 (1), 110-127. https://doi.org/10.1002/ppp.2038

Jones, B. M., Irrgang, A. M., Farquharson, L. M., Lantuit, H., Whalen, D., Ogorodov, S., Grigoriev, M., Tweedie, C., Gibbs, A. E., Strzelecki, M. C., Baranskaya, A., Belova, N., Sinitsyn, A., Kroon, A., Maslakov, A., Vieira, G., Grosse, G., Overduin, P., Nitze, I., Maio, C., Overbeck, J., Bendixen, M., Zagórski, P., Romanovsky, V.E. (2020). NOAA Arctic Report Card 2020, Coastal Permafrost Erosion, Administrative Report. https://doi.org/10.25923/E47W-DW52

Kääb, A., Strozzi, T., Bolch, T., Caduff, R., Trefall, H., Stoffel, M., & Kokarev, A. (2021). Inventory and changes of rock glacier creep speeds in Ile Alatau and Kungöy Ala-Too, northern Tien Shan, since the 1950s. The Cryosphere, 15(2), 927–949. https://doi.org/10.5194/tc-15-927-2021

Lissak, C., Bartsch, A., De Michele, M., Gomez, C., Maquaire, O., Raucoules, D., & Roulland, T. (2020). Remote Sensing for Assessing Landslides and Associated Hazards. Surveys in Geophysics, 41(6), 1391–1435. https://doi.org/10.1007/s10712-020-09609-1

Martin, L. C. P., Nitzbon, J., Scheer, J., Aas, K.S., Eiken, T., Langer, M., Filhol, S., Etzelmüller, B., & Westermann, S. (2021). Lateral thermokarst patterns in permafrost peat plateaus in northern Norway. The Cryosphere, 15, 3423–3442. https://doi.org/10.5194/tc-15-3423-2021

Nitze, I., Cooley, S. W., Duguay, C. R., Jones, B. M., & Grosse, G. (2020). The catastrophic thermokarst lake drainage events of 2018 in northwestern Alaska: Fast-forward into the future. The Cryosphere, 14(12), 4279–4297. https://doi.org/10.5194/tc-14-4279-2020

Nitze, I, Heidler, K., Barth, S., and Grosse, G. (submitted): Developing and testing a deep learning approach for mapping retrogressive thaw slumps. Remote Sensing.

Obu, J. (2021). How Much of the Earth's Surface is Underlain by Permafrost? Journal of Geophysical Research: Earth Surface, 126(5). https://doi.org/10.1029/2021JF006123

T. Popp, M.I. Hegglin, R. Hollmann, F. Ardhuin, A. Bartsch, A. Bastos, V. Bennett, J. Boutin, C. Brockmann, M. Buchwitz, E. Chuvieco, P. Ciais, W. Dorigo, D. Ghent, R. Jones, T. Lavergne, C.J. Merchant, B. Meyssignac, F. Paul, S. Quegan, S. Sathyendranath, T. Scanlon, M. Schröder, S.G.H. Simis, U. Willén (2020): Consistency of satellite climate data records for Earth system monitoring. Bulletin of the American Meteorological Society. https://doi.org/10.1175/BAMS-D-19-0127.1

Rouyet, L., Liu, L., Strand, S. M., Christiansen, H. H., Lauknes, T. R., & Larsen, Y. (2021). Seasonal InSAR Displacements Documenting the Active Layer Freeze and Thaw Progression in Central-Western Spitsbergen, Svalbard. Remote Sensing, 13(15), 2977. https://doi.org/10.3390/rs13152977

Runge, A. and Grosse, G. (2020): Mosaicking Landsat and Sentinel-2 Data to Enhance LandTrendr Time Series Analysis in Northern High Latitude Permafrost Regions. Remote Sensing, 12(15), 2471. https://doi.org/10.3390/rs12152471

Swingedouw, D., Ifejika Speranza, C., Bartsch, A., Durand, G., Jamet, C., Beaugrand, G., & Conversi, A. (2020). Early Warning from Space for a Few Key Tipping Points in Physical, Biological, and Social-Ecological Systems. Surveys in Geophysics, 41(6), 1237–1284. https://doi.org/10.1007/s10712-020-09604-6

Strozzi T., R.Caduff, N. Jones, C. Barboux, R, Delaloye, X. Bodin, A. Kääb, E. Mätzler, L. Schrott (2020). Monitoring Rock Glacier Kinematics with Synthetic Aperture Radar. Remote Sensing, 12(3), 559. https://doi.org/10.3390/rs12030559

Swingedouw, D., Speranza, C., Bartsch, A., Durand, G., Jamet, C., Beaugrand, G., Conversi, A. (2020): Early Warning from Space for a Few Key Tipping Points in Physical, Biological, and Social-Ecological Systems. Surveys in Geophysics. https://doi.org/10.1007/s10712-020-09604-6

Veremeeva, A., Nitze, I., Günther, F., Grosse, G., & Rivkina, E. (2021). Geomorphological and Climatic Drivers of Thermokarst Lake Area Increase Trend (1999–2018) in the Kolyma Lowland Yedoma Region, North-Eastern Siberia. Remote Sensing, 13(2), 178. https://doi.org/10.3390/rs13020178

Submitted/In review/In revision

Bartsch, A, Pointner, G., Nitze, I., Efimova, A., Jakober, D., Ley, S., Högström, E., Grosse, G., Schweitzer, P. (in revision): Expanding infrastructure and growing anthropogenic impacts along Arctic coasts. Environmental Research Letters.

Nitze, I, Heidler, K., Barth, S., and Grosse, G. (in review): "Developing and testing a deep learning approach for mapping retrogressive thaw slumps". Remote Sensing.

Runge, A., Nitze, I., & Grosse, G. (in revision). Remote Sensing Annual Dynamics of Rapid Permafrost Thaw Disturbances with LandTrendr. Remote Sensing of Environment.

5.2 News stories

IPA: Frozen Ground 43, the News Bulletin of the IPA, 2020
https://ipa.arcticportal.org/publications/frozen-ground

ESA
http://www.esa.int/Applications/Observing_the_Earth/Space_for_our_climate/Picturing_permafrost_in_the_Arctic

H2020 Nunataryuk
https://nunataryuk.org/news/139-new-map-shows-extent-of-permafrost-in-northern-hemisphere

Cover image of Permafrost and Periglacial Processes, volume 31, issue 3, July-September 2020, shows new permafrost map produced by UNEP Grid Arendal based on submarine permafrost map by Overduin et al. 2019 and land-based permafrost by Obu et al. 2019.

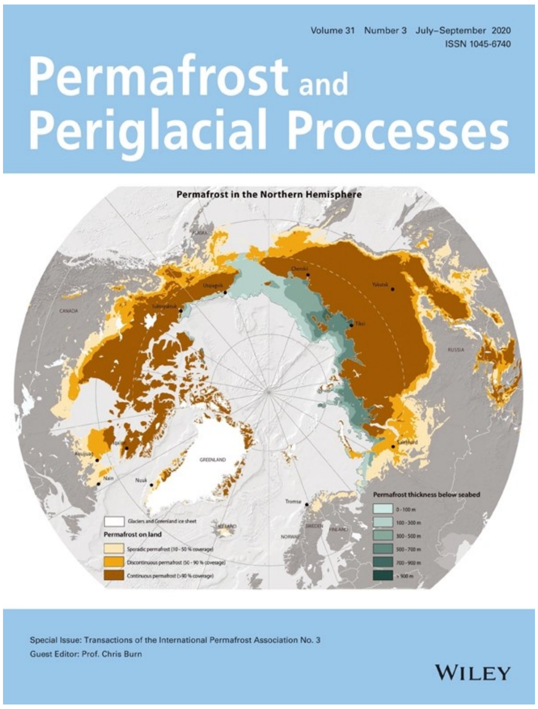

5.3 First user workshop

The first Permafrost_cci user workshop took place on September 27th 2021. It was held online with 66 participants. The project status was presented first. The first block of user presentations comprised climate modelling topics. The project use case #1 (HIRHAM) was presented by Heidrun Matthes (section 3.2). Kazuyuki Saito (YAMSTEC) discussed issues regarding soil organic carbon and ground ice dynamics in climate models. Eleanor Burke (Metoffice) showed a detailed assessment of permafrost_cci records with respect to CMIP6 activities. Ground temperature trends are similar to past records. This block was followed by planned and ongoing activities which combine or compare to other satellite products. This included an ESA fellowship presentation (A. Runge , AWI), use case #2 (Ingmar Nitze, AWI; section 3.3) and status of RECCAP-2 (Gustaf Hugelius, University Stockholm). The last user presentation block referred to applications of the permafrost extent product of DUE GlobPermafrost. Eventually, challenges in production and validation have been presented by Permafrost_cci team members. This covered lowland and mountain permafrost. The importance of validation in mountain areas and associated issues have been discussed. The need for documentation of how to work with the Polar Stereographic projection in GIS environment has been pointed out. In general there was positive feedback regarding the availability as NetCDF. The final discussion specifically addressed climate modelling applications. The following requirements have been stated:

- Monthly timesteps
- High vertical resolution (also 20 and 50 cm)
- Recommendations for aggregation/resampling to modelling grids

5.4 Outreach activities

- The Climate from Space application has been reviewed regarding the Permafrost component and feedback provided.
- For the WGClimate ECV Inventory, verification of Permafrost datasets (for publication in v3.0) has been provided to ECMWF.
- Permafrost_cci has been mentioned in an interview in BIORAMA #68 with A. Bartsch (in German).
- An ERL (Environmental Research Letters) special issue with focus on “Arctic Change: Transdisciplinary Research and Communication” has just been released (co-guest editor A. Bartsch). Topics include use of satellite observations in trans-disciplinary research and science communication.
- A summary of the project status has been published in the IPA bulletin #44.
- A news article from the CCI office regarding the release of the new permafrost_cci dataset with the title “Long-term permafrost record details Arctic thaw” was published by ESA on 16/12/2020, see https://www.esa.int/Applications/Observing_the_Earth/Space_for_our_climate/Long-term_permafrost_record_details_Arctic_thaw.
- An article about “How does Copernicus help understand the magnitude of permafrost thawing and its impacts on society and the environment?” was also published by Copernicus on 10/12/2020, see https://www.copernicus.eu/en/news/news/observer-how-does-copernicus-help-understandmagnitude-permafrost-thawing-and-its-impacts.
- A recording of a project presentation has been submitted for the CCI Knowledge exchange MOOC activity.
- The regional rock glacier inventories produced during the project are available online at https://www.unifr.ch/geo/geomorphology/en/research/cci-permafrost.html.

5.5 Presentations at scientific conferences

AGU 2020

- M. Wieczorek, B. Heim, S. Westermann, J. Obu, U. Herzschuh, F.M. Seifert, T. Strozzi, and A. Bartsch, Comparison of in situ ground temperatures and active layer depths with the ESA CCI+ Permafrost Mean Annual Temperature and Active Layer Thickness products (poster);
- A. Bartsch, G. Pointner, T. Ingeman-Nielsen and W. Lu, Progress in monitoring landcover and human presence in the Arctic based on satellite data (oral);
- I. Nitze, B. Jones, A. Veremeeva, S. Westermann, A. Bartsch, V. Romanovsky and G. Grosse, Permafrost region disturbances in space and time: a pan-arctic perspective (oral);

- B. Heim, I. Shevtsova, A. Runge, S. Kruse, I. Nitze, G. Grosse, U. Herzschuh, A. Buchwal, G. Rachlewicz and A. Bartsch, Remote Sensing approaches for assessing vegetation carbon stocks and fluxes in the Lena River Delta (Northern Yakutia, Russia) (oral).

Arctic Change 2020

- A. Bartsch & ESA DUE Globpermafrost & CCI+ Permafrost Team, Arctic change revealed by satellite - Data collections of ESA DUE GlobPermafrost and ESA CCI+ Permafrost (eposter);
- A. Bartsch, G. Pointner, T. Ingeman-Nielsen and W. Lu, Progress in detection and monitoring of transportation infrastructure in the Arctic based on satellite data (oral).

ASSW 2021

- Bartsch et al. Monitoring of infrastructure across the Arctic with Sentinel-1 and -2. RATIC workshop: RATIC meets T-MOSAiC: Sharing Best Practices in Research on Infrastructures in the Arctic. ASSW 2021, 21.03.2021 (presentation, use case)
- Bartsch et al. Arctic change revealed by satellite - Data collections of ESA DUE GlobPermafrost and ESA CCI+ Permafrost. Session: ID:91 - Arctic in Transition: Monitoring Ecosystem Change from the Ground, Air, and Space. ASSW 2021, 25.03.2021 (poster)
- Bartsch et al. Arctic change revealed by satellite - Data collections of ESA DUE GlobPermafrost and ESA CCI+ Permafrost. International Symposium “Focus Siberian Permafrost – Terrestrial Cryosphere and Climate Change”, 25.3.2021 (poster)

EGU 2021

- Bertone, A., Barboux, C., Brardinoni, F., Delaloye, R., Mair, V., Pellegrinon, G., Monier, T., and Strozzi, T.: A complementary kinematic approach to inventory rock glaciers applied to case studies of the Swiss and Italian Alps, EGU General Assembly 2021, online, 19–30 Apr 2021, EGU21-14661, https://doi.org/10.5194/egusphere-egu21-14661, 2021.
- Jakober, D., Bergstedt, H., Kroisleitner, C., and Bartsch, A.: Comparison of permafrost mean annual ground temperature derived from two different satellite-based schemes: land surface temperature based (ESA CCI+ Permafrost) versus surface status (Metop ASCAT), EGU General Assembly 2021, online, 19–30 Apr 2021, EGU21-9824, https://doi.org/10.5194/egusphereegu21-9824, 2021.

EO Polar Science Week

- e-poster about validation of permafrost_cci datasets by Birgit Heim
- Presentation by A. Bartsch in the NASA/ESA evening permafrost and methane session: 'Monitoring wet versus dry across the Arctic'
- Presentation by A. Bartsch in land session (also chair): 'Introduction : advances in recent projects and initiatives'
- Session chair A. Bartsch for 2nd session of the the NASA/ESA evening permafrost and methane initiative
- Presentation by A. Bartsch in Freshwater flux session: 'EO challenges for monitoring ice and water in the ground across the Arctic'
- e-poster about the current project status by Tazio Strozzi

- Several related tweets were sent out by the climate office

FRINGE 2021

- Line Rouyet, Lin Liu, Tom Rune Lauknes, Hanne Christiansen, Hanne Hvidtfeldt, Sarah Strand and Yngvar Larsen, Mapping the timing of seasonal thaw subsidence maxima in central Western Spitsbergen, 11th International Workshop on "Advances in the Science and Applications of SAR Interferometry and Sentinel-1 InSAR" (Fringe 2021), 31 May - 4 June 2021.
-

Other

- Bartsch, A., Ley, S., Pointner G., Nitze I., Vieira G: ALOS PALSAR & PALSAR2 applicability for Arctic coastal erosion monitoring. Poster at the Joint PI Meeting of the JAXA Earth Observation Missions FY2020, January 2021 (use case presentation).
- Project presentation at the May CMUG meeting on 07.05.2021(A. Bartsch).
- Presentation of Permafrost_cci requirements at the Snow_cci user workshop on 25.05.2021 (S.Westermann).
- Line Rouyet, Integration of geomorphological mapping and InSAR kinematics for a comprehensive inventory of rock glaciers in Nordenskiöld Land, SIOS Online Conference on "Earth Observation (EO)andRemote Sensing (RS) applications in Svalbard", 08-10 June 2021.
- Grosse, G. (2021): Arctic Change and Permafrost. Presentation during the digital event series "Climate Change and Security in the Arctic" organized by the Konrad Adenauer Foundation (KAS) to strengthen the cooperation between the Nordic countries and Germany on Arctic issues and to promote a common understanding for the development of a common European Arctic policy. 07 September, 2021.
- Matthes et al., ESA CCI+ Permafrost, Data sets and application.Polar CORDEX meeting, October 5-7 2020, online

Upcoming Events

Regional Conference on Permafrost, 24-29 October 2021, online.

- M. Darrow, R. Caduff, R. Daanen, L. Arenson, C. Barboux, R. Delaloye and T. Strozzi, Comparing Slope Movement Rates in the Brooks Range, Alaska, USA, 2021 Regional Conference on Permafrost (RCOP 2021).
- Matthes et al., Uncertainties from land surface boundary conditions: atmosphere and cryosphere present day representation in a Regional Arctic Climate Model, USA, 2021 Regional Conference on Permafrost (RCOP 2021).
- Nitze et al, Evaluating a deep-learning approach for mapping retrogressive thaw slumps across the Arctic
- Lambiel et al., Distribution and kinematics of rock glaciers in the Southern Alps of New Zealand.

- Manconi et al., Systematic monitoring of rock glacier kinematics from satellite SAR interferometry: insights from case studies in the European Alps and Disko Island.
- Bartsch et al., Infrastructure monitoring and combination with permafrost_cci records
- Grosse et al.., Airborne Surveys of Rapidly Changing Permafrost Landscapes in Western Alaska
- Runge et al., Permafrost Vulnerability Framework from multiple Essential Climate Variables
- Bartsch et al., The potential of satellite data to identify and quantify permafrost presence and change
- Pellet et al., Permafrost warming in the Swiss Alps: current state and long-term trends
- Pellet et al., Operational monitoring of rock glacier kinematics: insights from the PERMOS network
- Strozzi et al., Systematic monitoring of rock glacier kinematics from satellite SAR interferometry: insights from case studies in the European Alps and Disko Island
- Bartsch et al, A spatially consistent account of infrastructure across the entire Arctic

AGU Fall Meeting 2021

- Nitze et al., Evaluating a deep-learning approach for mapping retrogressive thaw slumps across the Arctic
- Nitze et al., How to discover an unknown mega-landslide in the Siberian far-east

Further Conferences/Meetings

Grosse, G. et al.: Permafrost Change in a Rapidly Warming Arctic. 8th transdisciplinary Workshop "Gateway to the Arctic". 4 October 2021, Potsdam, Germany.

Grosse, G. et al.: Space-Based Observations of Dynamic Arctic Permafrost Landscapes. Deutsch-Russische Konferenz „Anpassung der Umwelt Sibiriens an den Klimawandel: Ökologische und soziale Aspekte“. 6-7 October 2021, Tomsk, Russia.

Grosse, G. et al.: Remote Sensing of Permafrost Change in the Arctic. Conference on Cryosphere Transformation & Geotechnical Safety. 8-12 November 2021, Salekhard, Russia.

5.6 Specific tasks

Session chairing:
ASSW 2021
A.Bartsch and I.Nitze co-chaired the Remote Sensing Session at ASSW 2021
M.Wieczoreck co-chaired the Session Progress Towards Realizing Data Sharing for the Arctic Region and Beyond at ASSW 2021

RCOP 2021
I. Nitze will co-chair the Permafrost Discovery Gateway session/workshop

Conference organization:
G. Grosse is member of the International Scientific Committee of the 16th International Circumpolar Remote Sensing Symposium (ICRSS) (Postponed to May 2022, Fairbanks, Alaska)

5.7 Student teaching and courses

Remote Sensing of Permafrost Regions, MSc Module taught by G. Grosse & I. Nitze at University of Potsdam (4 hrs/week; SS 2019, WS 2019/2020, WS 2020/2021, WS 2021/2022)

HEIBRiDS Seminar Series. I.Nitze: Machine-learning for mapping permafrost landscape dynamics. https://www.heibrids.berlin/

Potsdam Summer School 2021. I.Nitze: Wetting vs. Drying of Arctic Permafrost landscapes. https://potsdam-summer-school.org/

6 REFERENCES

6.1 Bibliography

Bartsch, A.; Höfler, A.; Kroisleitner, C.; Trofaier, A.M. 2016: Land Cover Mapping in Northern High Latitude Permafrost Regions with Satellite Data: Achievements and Remaining Challenges. Remote Sens., 8, 979.

Bartsch A., Ley S., Nitze I, Pointner G. and Vieira G. (2020) Feasibility Study for the Application of Synthetic Aperture Radar for Coastal Erosion Rate Quantification Across the Arctic. Front. Environ. Sci. 8:143. doi: 10.3389/fenvs.2020.00143

Biskaborn, B. K., Lanckman, J.-P., Lantuit, H., Elger, K., Streletskiy, D. A., Cable, W. L., & Romanovsky, V. E. (2015). The new database of the Global Terrestrial Network for Permafrost (GTN-P). Earth System Science Data, 7(2), 245–259. https://doi.org/10.5194/essd-7-245-2015

Biskaborn, B.K., Smith, S.L., Noetzli, J., Matthes, H., Vieira, G., Streletskiy, D.A., Schoeneich, P., Romanovsky, V.E., Lewkowicz, A.G., Abramov, A. and Allard, M., 2019. Permafrost is warming at a global scale. Nature Communications, 10(1), p.264.

Brown R.J.E., 1970: Permafrost in Canada: Its influence on northern development. University of Toronto Press, Toronto 234 p.

Cable, W.L.; Romanovsky, V.E.; Jorgenson, M.T., 2016: Scaling-up permafrost thermal measurements in western Alaska using an ecotype approach. Cryosphere, 10, 2517–2532.

Chadburn, S., Burke, E., Cox, P., Friedlingstein, P., Hugelius, G., Westermann, S., 2017a: An observation-based constraint on permafrost loss as a function of global warming, Nature Climate Change, doi:10.1038/nclimate3262.

Chadburn, S. E., Krinner, G., Porada, P., Bartsch, A., Beer, C., Belelli Marchesini, L., Boike, J., Ekici, A., Elberling, B., Friborg, T., Hugelius, G., Johansson, M., Kuhry, P., Kutzbach, L., Langer, M., Lund, M., Parmentier, F.-J. W., Peng, S., Van Huissteden, K., Wang, T., Westermann, S., Zhu, D., and Burke, E. J., 2017b: Carbon stocks and fluxes in the high latitudes: using site-level data to evaluate Earth system models, Biogeosciences, 14, 5143-5169, https://doi.org/10.5194/bg-14-5143-2017.

Christensen, O. B., M. Drews, J. H. Christensen, K. Dethloff, K. Ketelsen, I. Hebestadt, and A. Rinke (2007), The HIRHAM regional climate model, version 5, Tech. Rep. 06-17, Dan. Meteorol. Inst., Copenhagen, http://www.dmi.dk/dmi/tr06-17.pdf.

Gisnås, K., Westermann, S., Schuler, T. V., Litherland, T., Isaksen, K., Boike, J., and Etzelmüller, B.: A statistical approach to represent small-scale variability of permafrost temperatures due to snow cover, 2014: The Cryosphere, 8, 2063-2074, https://doi.org/10.5194/tc-8-2063-2014.

Grosse G., Robinson J.E., Bryant R., Taylor M.D., Harper W., DeMasi A., Kyker-Snowman E., Veremeeva A., Schirrmeister L., Harden J. (2013): Distribution of late Pleistocene ice-rich syngenetic permafrost of the Yedoma Suite in east and central Siberia, Russia. U.S. Geological Survey Open File Report 2013-1078, 37p.

Heginbottom, J.A., 1984: The mapping of permafrost. Canadian Geographer, Vol. 28, No.1, pp. 78-83.

Heginbottom, J.A., Radburn, L.K., 1992: Permafrost and Ground Ice Conditions of Northwestern Canada (Mackenzie Region). National Snow and Ice Data Center, Boulder, CO, USA.

IPCC, 2013: Climate Change 2013: The Physical Science Basis. Contribution of Working Group I to the Fifth Assessment Report of the Intergovernmental Panel on Climate Change [Stocker, T.F., D. Qin, G.-K. Plattner, M. Tignor, S.K. Allen, J. Boschung, A. Nauels, Y. Xia, V. Bex and P.M. Midgley (eds.)]. Cambridge University Press, Cambridge, United Kingdom and New York, NY, USA, 1535 pp.

IPCC, 2019: IPCC Special Report on the Ocean and Cryosphere in a Changing Climate (SROCC).

IPCC, 2021: Climate Change 2021: The Physical Science Basis. Contribution of Working Group I to the Sixth Assessment Report of the Intergovernmental Panel on Climate Change [Masson-Delmotte, V., P. Zhai, A. Pirani, S.L. Connors, C. Péan, S. Berger, N. Caud, Y. Chen, L. Goldfarb, M.I. Gomis, M. Huang, K. Leitzell, E. Lonnoy, J.B.R. Matthews, T.K. Maycock, T. Waterfield, O. Yelekçi, R. Yu, and B. Zhou (eds.)]. Cambridge University Press. In Press.

Jones, B. M., Kolden, C. A., Jandt, R., Abatzoglou, J. T., Urban, F., & Arp, C. D. (2009). Fire Behavior, Weather, and Burn Severity of the 2007 Anaktuvuk River Tundra Fire, North Slope, Alaska. Arctic, Antarctic, and Alpine Research, 41(3), 309–316. https://doi.org/10.1657/1938-4246-41.3.309

Kelley, A. M., Epstein, H. E., and Walker, D. A., 2004: Role of vegetation and climate in permafrost active layer depth in arctic tundra of northern Alaska and Canada, J. Glaciol. Climatol., 26, 269–273.

Koven, C.D., W.J. Riley, and Stern, A., 2013: Analysis of Permafrost Thermal Dynamics and Response to Climate Change in the CMIP5 Earth System Models. J. Climate, 26, 1877–1900

Kudryavtsev V.A., (Editor) 1978: Obshcheye merzlotovedeniya (Geokriologiya) (General permafrost science) In Russian. Izd. 2, (Edu 2) Moskva (Moscow), Izdatel'stvo Moskovskogo Universiteta, (Moscow University Editions), 404 p

Matthes, H., Rinke, A. and Dethloff, 2015: K.,Recent changes in Arctic temperature extremes: warm and cold spells during winter and summer, Environmental Research Letters, 10(11).

Matthes, H., Rinke, A., Zhou, X., and Dethloff, K., 2017: Modelling atmosphere and permafrost in the Arctic using a new regional coupled atmosphere-land model, Journal of Geophysical Research Atmospheres, 122, 7755–7771.

McGuire AD, Koven C, Lawrence DM, Clein JS, Xia J, Beer C, Burke E, Chen G, Chen X, Delire C, Jafarov E, MacDougall AH, Marchenko S, Nicolsky D, Peng S, Rinke A, Saito K, Zhang W, Alkama R, Bohn TJ, Ciais P, Decharme B, Ekici A, Gouttevin I, Hajima T, Hayes DJ, Ji D, Krinner G, Lettenmaier DP, Luo Y, Miller PA, Moore JC, Romanovsky V, Schädel C, Schaefer K, Schuur EAG, Smith B, Sueyoshi T, Zhuang Q, 2016: Variability in the sensitivity among model simulations of permafrost and carbon dynamics in the permafrost region between 1960 and 2009, 2016: Global Biogeochemical Cycles. doi:10.1002/2016GB005405

Muller S.W, 1943: Permafrost or permanently frozen ground and related engineering problems. U.S. Engineers Office, Strategic Engineering Study, Special Report No. 62. 136p. (Reprinted in 1947, J. W. Edwards, Ann Arbor, Michigan, 231p.)

Nelson, F. E., Shiklomanov, N. I., Mueller, G. R., Hinkel, K. M., Walker, D. A., and Bockheim, J. G., 1997: Estimating Active-Layer Thickness over a Large Region: Kuparuk River Basin, Alaska, USA, Arctic Alpine Res., 29, 4, doi:10.2307/1551985.

Nitze, I., Grosse, G., Jones, B. M., Arp, C. D., Ulrich, M., Fedorov, A., & Veremeeva, A. (2017). Landsat-based trend analysis of lake dynamics across northern permafrost regions. Remote Sensing, 9(7), 640.

Nitze, I., Grosse, G., Jones, B. M., Romanovsky, V. E., & Boike, J. (2018a). Remote sensing quantifies widespread abundance of permafrost region disturbances across the Arctic and Subarctic. Nature communications, 9(1), 1-11.

Nitze, I., Grosse, G., Jones, B. M., Romanovsky, V. E., & Boike, J. (2018b). Data Documentation v1. 0: Remote sensing quantifies widespread abundance of permafrost region disturbances across the Arctic and Subarctic.

Nitze, I., Cooley, S., Duguay, C., Jones, B. M., & Grosse, G. (2020). The catastrophic thermokarst lake drainage events of 2018 in northwestern Alaska: Fast-forward into the future. The Cryosphere Discussions, 1-33.

Obu, J., Westermann, S., Kääb, A., & Bartsch, A. (2018). Ground Temperature Map, 2000-2016, Northern Hemisphere Permafrost (p. 40 data points) [Text/tab-separated-values]. PANGAEA - Data Publisher for Earth & Environmental Science. https://doi.org/10.1594/PANGAEA.888600

Obu, J., Westermann, S., Bartsch, A., Berdnikov, N., Christiansen, H.H., Dashtseren, A., Delaloye, R., Elberling, B., Etzelmüller, B., Kholodov, A. and Khomutov, A., 2019. Northern Hemisphere permafrost map based on TTOP modelling for 2000–2016 at 1 km2 scale. Earth-Science Reviews.

Obu, J. (2021). How Much of the Earth's Surface is Underlain by Permafrost? Journal of Geophysical Research: Earth Surface, 126(5). https://doi.org/10.1029/2021JF006123

Romanovsky, V. E., Smith, S. L., & Christiansen, H. H. (2010). Permafrost thermal state in the polar Northern Hemisphere during the international polar year 2007–2009: A synthesis. Permafrost and Periglacial Processes, 21(2), 106–116.

Schaefer K, Lantuit H, Romanovsky VE, Schuur EAG, Witt R, 2014: The impact of the permafrost carbon feedback on global climate. Environmental Research Letters, 9, 085003.

Strauss J, Schirrmeister L, Grosse G, Fortier D, Hugelius G, Knoblauch C, Romanovsky VE, Schädel C, Schneider von Deimling T, Schuur EAG, Shmelev D, Ulrich M, Veremeeva A. (2017): Deep Yedoma permafrost: A synthesis of depositional characteristics and carbon vulnerability. Earth-Science Reviews, 172: 75-86. doi: 10.1016/j.earscirev.2017.07.007

Schuur EA, McGuire AD, Schädel C, Grosse G, Harden JW, Hayes DJ, Hugelius G, Koven CD, Kuhry P, Lawrence DM, Natali SM., 2015: Climate change and the permafrost carbon feedback. Nature. Apr;520(7546):171.

Slater, A.G. and D.M. Lawrence, 2013: Diagnosing Present and Future Permafrost from Climate Models. J. Climate, 26, 5608–5623, https://doi.org/10.1175/JCLI-D-12-00341.1

Strauss J, Schirrmeister L, Grosse G, Fortier D, Hugelius G, Knoblauch C, Romanovsky VE, Schädel C, Schneider von Deimling T, Schuur EAG, Shmelev D, Ulrich M, Veremeeva A. (2017): Deep Yedoma permafrost: A synthesis of depositional characteristics and carbon vulnerability. Earth-Science Reviews, 172: 75-86. doi: 10.1016/j.earscirev.2017.07.007

Turetsky, M. R., Abbott, B. W., Jones, M. C., Walter Anthony, K., Olefeldt, D., Schuur, E. A. G., Koven, C., McGuire, A. D., Grosse, G., Kuhry, P., Hugelius, G., Lawrence, D. M., Gibson, C., & Sannel, A. B. K. (2019). Permafrost collapse is accelerating carbon release. Nature, 569(7754), 32–34. https://doi.org/10.1038/d41586-019-01313-4

Vincent, W.F., Lemay, M. and Allard, M., 2017. Arctic permafrost landscapes in transition: towards an integrated Earth system approach. Arctic Science, 3(2), pp.39-64.

Westermann, S., Østby, T., Gisnås, K., Schuler.T., Etzelmüller, B., 2015: A ground temperature map of the North Atlantic permafrost region based on remote sensing and reanalysis data, The Cryosphere, 9, 1303-1319, doi:10.5194/tc-9-1303-2015.

Williams, J.R., 1965: Ground water in permafrost regions: An annotated bibliography. U.S. Geological Survey, Professional Paper 696, 83p.

Windirsch, T., Grosse, G., Ulrich, M., Schirrmeister, L., Fedorov, A. N., Konstantinov, P. Y., Fuchs, M., Jongejans, L. L., Wolter, J., Opel, T., and Strauss, J.: Organic carbon characteristics in ice-rich permafrost in alas and Yedoma deposits, central Yakutia, Siberia, Biogeosciences, 17, 3797–3814, https://doi.org/10.5194/bg-17-3797-2020, 2020.

van Everdingen R.O., 1985: Unfrozen permafrost and other taliks. Workshop on Permafrost Geophysics, Golden, Colorado, October 1984 (J. Brown, M.C. Metz, P. Hoekstra, Editors). U.S. Army, C.R.R.E.L., Hanover, New Hampshire, Special Report 85-5, pp.101-105

6.2 Acronyms

ACOP	Asian Conference on Permafrost
ALT	Active Layer Thickness
Arctic CORDEX	Coordinated Regional Climate Downscaling Experiment
ASSW	Arctic Science Summit Week
AWI	Alfred Wegener Institute Helmholtz Centre for Polar and Marine Research
B.GEOS	b.geos GmbH
CALM	Circumpolar Active Layer Monitoring
CliC	Climate and Cryosphere project
CLM4	Land Community Model Version 4
CLM5	Land Community Model Version 5
CCI	Climate Change Initiative
CMIP-6	The Coupled Model Intercomparison Project
CMUG	Climate Modelling User Group
CRESCENDO	Coordinated Research in Earth Systems and Climate: Experiments, Knowledge, Dissemination and Outreach
CRG	Climate Research Group
ECV	Essential Climate Variable
EO	Earth Observation
ESA	European Space Agency
ESA DUE	ESA Data User Element
FT2T	Freeze-Thaw to Temperature
GAMMA	Gamma Remote Sensing AG
GCOS	Global Climate Observing System

GCW	Global Cryosphere Watch
GTD	Ground Temperature at certain depth
GT	Ground Temperature
GTN-P	Global Terrestrial Network for Permafrost
GTOS	Global Terrestrial Observing System
GUIO	Department of Geosciences University of Oslo
HIRHAM	High Resolution Limited Area Model
HRPC	Hot Spot Regions of Permafrost Change
IASC	International Arctic Science Committee
ILAMB	International Land Model Benchmarking
IPA	International Permafrost Association
IPCC	Intergovernmental Panel on Climate Change
LS3MIP	Land Surface, Snow and Soil Moisture
MAGT	Mean Annual Ground Temperature
NetCDF	Network Common Data Format
NSIDC	National Snow and Ice Data Center
PCN	Permafrost Carbon Network
PE	Permafrost Extent
PERMOS	Swiss Permafrost Monitoring Network
PF	Permafrost
PFR	Permafrost Fraction
PSTG	Polar Space Task Group
PUG	Product User Guide
PVIR	Product Validation and Intercomparison Report
RASM	Regional Arctic System Model
RCOP	Regional Conference on Permafrost
RD	Reference Document
RMSE	Root Mean Square Error
RS	Remote Sensing
SAR	Synthetic Aperture Radar
SCAR	Scientific Committee on Antarctic Research
SU	Department of Physical Geography Stockholm University
TSP	Thermal State of Permafrost
UNIFR	Department of Geosciences University of Fribourg
URD	Users Requirement Document
WCRP	World Climate Research Program
WMO	World Meteorological Organisation
WMO OSCAR	Observing Systems Capability Analysis and Review Tool
WUT	West University of Timisoara